Nuclear Physics B282 (1987) 253–307
North-Holland, Amsterdam

PROBING THE WEAK BOSON SECTOR IN $e^+e^- \to W^+W^-$

K. HAGIWARA[1], R.D. PECCEI and D. ZEPPENFELD[2]

DESY, Theory Group, D-2000 Hamburg 52, Fed. Rep. Germany

K. HIKASA[3]

Physics Department, University of Wisconsin, Madison, Wisconsin 53706, USA

Received 23 June 1986

A detailed analysis of W pair production in e^+e^- annihilation at LEP-II energies is presented by using helicity amplitudes for the process $e^+e^- \to W^+W^-$ with arbitrary $WW\gamma$ and WWZ couplings. Expressing the complete angular distribution of W decay products in terms of these helicity amplitudes, we perform a systematic search for the most sensitive angular distributions or correlations for anomalous couplings. As a result precise tests of the gauge-theory cancellations between different diagrams are suggested. Angular distributions sensitive to W^+W^- rescattering effects and/or *CP*-violating vector boson couplings are studied as well. Complete helicity amplitudes for the process $e^+e^- \to W^+W^- \to (q_1\bar{q}_2g)(q_3\bar{q}_4g)$ with arbitrary quark masses and finite W width are presented in a form convenient for their direct numerical evaluation. Amplitudes for the processes $e^+e^- \to ZZ$ and $Z\gamma$ are also included.

1. Introduction

The prime target of experiments at LEP in its second phase (LEP-II) is the production of charged weak boson (W) pairs in e^+e^- annihilation [1–33]. The production cross section reaches its maximum (~ 20 pb) at $\sqrt{s} \sim 200$ GeV and one expects to observe 10^4 W pairs a year with the design luminosity of 5×10^{31} $cm^{-2}\,sec^{-1}$. Detailed quantitative tests of electroweak theories should thus be possible at LEP-II.

There are two distinctive aspects of W pair production studies in e^+e^- annihilation [1]. First, a precise determination of the W boson properties, e.g., its mass, width, and its couplings to different quark flavors (Cabibbo-Kobayashi-Maskawa

[1] Address after July 1986: KEK, Tsukuba, Ibaraki 305, Japan.
[2] Address after October 1986: Physics Department, University of Wisconsin, Madison, Wisconsin 53706, USA.
[3] Address after October 1986: KEK, Tsukuba, Ibaraki 305, Japan.

0550-3213/87/$03.50

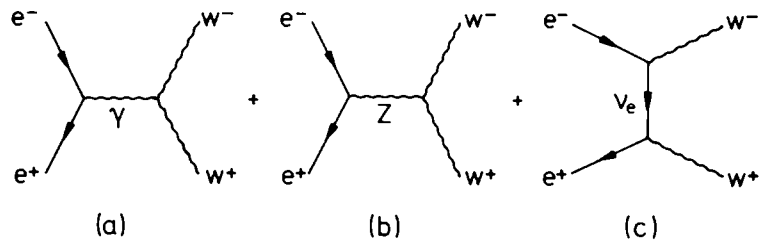

Fig. 1. Feynman diagrams for the process $e^+e^- \to W^+W^-$.

matrix elements) can be achieved in the clean environment of e^+e^- annihilation. A precise measurement of m_W is particularly important [1, 34] to test the standard theory of electroweak unification a the loop level. Second, this process provides the best opportunity to measure directly the three-vector-boson couplings, WWγ and WWZ, via s-channel γ and Z exchange contributions (see fig. 1). Indeed, the requirement of tree unitarity for the process $e^+e^- \to W^+W^-$ restricts uniquely the three-vector-boson couplings to the form prescribed by the Yang-Mills self-interaction [35]. In other words, a small deviation of these couplings from their gauge theory values violates the subtle cancellation among the three contributions shown in fig. 1 and hence can lead to observable effects. We shall see in the following that the sensitivity to these couplings in the process $e^+e^- \to W^+W^-$ is far greater than that achievable at $Sp\bar{p}S$ or the Tevatron collider by W pair production [11, 36–38], Wγ production [36, 39], and W radiative decay [39] processes* even at the moderate energies reachable at LEP-II.

A number of authors have made important contributions to the subject. Charged vector boson pair production in e^+e^- collision was examined already in 1961 by Cabibbo and Gatto [2, 3], and these papers were followed by several studies [4, 5, 7]. Dolgov and Solov'ev [6] were the first to include the weak (ν exchange) contribution in 1965.

In contrast to these early results, the amplitude for $e^+e^- \to W^+W^-$ in spontaneously broken gauge theories was shown [41] to have good high-energy behavior. The converse was also shown to hold: good high-energy behavior singled out gauge theories [35]. After the opening of the gauge theory era, the process received more intensive investigation.

The cross section in the standard $SU(2) \otimes U(1)$ theory was calculated by many authors. The total cross section was first calculated by Sushkov, Flambaum, and Khriplovich [8]. Alles, Boyer, and Buras [9] presented the differential cross section and displayed the gauge-theory cancellation. Bletzacker and Nieh [10] included transverse beam polarization and numerically calculated various distributions including the final lepton energy and lepton-beam angle distributions, the azimuthal-

* See also ref. [40] for W pair production studies in hadron collisions.

angle correlation between the two final leptons, and the average dilepton mass. The analytic form of the lepton energy and angle distributions was obtained by Mery and Perrottet [15]. Koval'chuk, Rekalo, and Stoletnii [25], studied the energy-angle distributions of the lepton, while the double energy distributions of the two final leptons were examined by Dicus and Kallianpur [28]. Duncan, Kane, and Repko [29] showed that a certain azimuthal-angle correlation of two decay planes is very small in the standard model.

Meanwhile, the density matrix for single W polarization was derived by Koval'chuk and Rekalo [14], and the ratio of the three helicity states was calculated by Bilchak, Brown, and Stroughair [22]. The one-loop radiative corrections to the process were evaluated by Lemoine and Veltman [13] and by Philippe [17]. Without explicitly referring to the "intermediate" W state, the process can be described in terms of the initial and final fermions. The helicity amplitudes in this approach (which is different from ours) were calculated by Kleiss [31] and by Gunion and Kunszt [32].

W-pair production in extended nongauge models has also been studied. The polarization amplitudes with the most general three-vector-boson couplings were presented by Gaemers and Gounaris [12]. However, most studies of these anomalous couplings restricted themselves to just a few couplings which satisfy C, P, and T invariance separately. The effect of these nongauge terms was examined in the differential and total cross section [21, 26, 30], the single W helicity ratios [22], the lepton-beam angular distribution [26], and in the single and double lepton energy distributions [28].

The purpose of this paper is to systematize these previous studies. First, we will present a general expression for the distribution of the decay products of the two W's in terms of the $e^+e^- \to W^+W^-$ helicity amplitudes. Then we will study the effects of various possible anomalous three-vector-boson couplings in detail.

The paper is organized as follows. In sect. 2, we give the most general form of the $WW\gamma$ and WWZ couplings and show which constraints on these couplings come from electroweak gauge symmetry, C, P, and electromagnetic U(1) gauge invariance. This section updates the work of Gaemers and Gounaris [12]. In sect. 3, we present the complete helicity amplitudes for the process $e^-e^- \to W^+W^-$ in a compact form, making the gauge-theory cancellation between γ, Z, and ν exchange graphs manifest. These amplitudes are derived for the most general couplings of the previous section. Sect. 4 presents all 81 coefficients of the quadri-differential angular distributions of the W^+ and W^- decays into massless fermion pairs, expressed in terms of the helicity amplitudes for W pair production. Sect. 5 gives the main results of this paper, which are angular distributions and correlations of W decay products providing tests of the three-vector-boson couplings. In this section the separation of longitudinally polarized W's from transversely polarized W's, polar and azimuthal angle distributions of W decay products, and also correlations between W^+ and W^- decays are studied systematically. Finally sect. 6 gives a summary and some conclusions.

We include four appendices for completeness. In appendix A, we show that only seven of the nine form factors given by Gaemers and Gounaris are independent. In appendix B, the twofold solutions for the neutrino momenta in the process $e^+e^- \to W^+W^- \to (\ell^+\nu)(\ell^-\bar{\nu})$ is explicitly given in terms of the observable charged lepton momenta, in the zero W width limit. In appendix C, we provide a closed expression for the helicity amplitudes for W pair production, followed by decays of each W into massive fermion pairs with or without a single gluon emission. Here we include finite W width effects since they are necessary for a precise measurement of m_W and for flavor identification [1]. The helicity amplitudes are expressed in a formalism developed by two of us [42], which makes their direct numerical evaluation simple and efficient. Finally, appendix D gives helicity amplitudes for the processes $e^+e^- \to ZZ$ and $Z\gamma$.

2. Three-vector-boson couplings

The general couplings of two charged vector bosons with a neutral vector boson, $WW\gamma$ and WWZ, can be derived from the following effective lagrangian*

$$\begin{aligned}\mathscr{L}_{WWV}/g_{WWV} = {} & ig_1^V\left(W_{\mu\nu}^\dagger W^\mu V^\nu - W_\mu^\dagger V_\nu W^{\mu\nu}\right) + i\kappa_V W_\mu^\dagger W_\nu V^{\mu\nu} \\ & + \frac{i\lambda_V}{m_W^2} W_{\lambda\mu}^\dagger W^\mu{}_\nu V^{\nu\lambda} - g_4^V W_\mu^\dagger W_\nu\left(\partial^\mu V^\nu + \partial^\nu V^\mu\right) \\ & + g_5^V \varepsilon^{\mu\nu\rho\sigma}\left(W_\mu^\dagger \overleftrightarrow{\partial}_\rho W_\nu\right) V_\sigma + i\tilde{\kappa}_V W_\mu^\dagger W_\nu \tilde{V}^{\mu\nu} \\ & + \frac{i\tilde{\lambda}_V}{m_W^2} W_{\lambda\mu}^\dagger W^\mu{}_\nu \tilde{V}^{\nu\lambda}. \end{aligned} \tag{2.1}$$

Here $V^\mu (= V^{\mu\dagger})$ stands for either the photon or the Z field, corresponding to $V = \gamma$ or Z respectively, W^μ is the W^- field, $W_{\mu\nu} = \partial_\mu W_\nu - \partial_\nu W_\mu$, $V_{\mu\nu} = \partial_\mu V_\nu - \partial_\nu V_\mu$, $\tilde{V}_{\mu\nu} = \frac{1}{2}\varepsilon_{\mu\nu\rho\sigma}V^{\rho\sigma}$, and $(A\overleftrightarrow{\partial}_\mu B) = A(\partial_\mu B) - (\partial_\mu A)B$.

The seven operators** in (2.1) exhaust all possible Lorentz structure when we neglect the scalar component of all three-vector-bosons:

$$\partial_\mu V^\mu = 0, \qquad \partial_\mu W^\mu = 0. \tag{2.2}$$

* Throughout the paper, we use the Bjorken-Drell metric with $\varepsilon_{0123} = -\varepsilon^{0123} = +1$.

** Seven operators are sufficient due to the fact that only seven out of the nine helicity states of the W pair can be reached by s-channel vector boson exchange ($J = 1$ channel). The other two helicity combinations have both W spins pointing in the same direction and thus have $J \geqslant 2$.

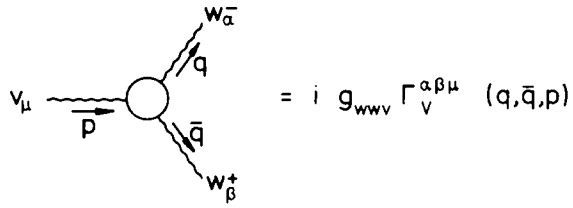

Fig. 2. Feynman rule for the general WWV (V = γ or Z) vertices.

This condition is automatic for on-shell W's:

$$\left(\Box + m_W^2\right) W^\mu = 0, \qquad \partial_\mu W^\mu = 0. \tag{2.3}$$

It also holds for the virtual photon and is valid for the Z in the process we are investigating. Terms containing $\partial_\mu Z^\mu$ are in fact proportional to the electron mass and negligible.

The lagrangian (2.1) contains 5 operators with dimension four and 2 with dimension six. All the higher-dimensional operators for on-shell W's are obtained from the operators in eq. (2.1) simply by replacing V^μ by $\Box^n V^\mu$ ($\Box = \partial^2$) with an arbitrary positive integer n. These operators form a complete set* of WWV couplings under the conditions (2.2) and (2.3). Any other operator can be reduced to a combination of these**.

In momentum space as depicted in fig. 2, the corresponding WWV vertex can be expressed as follows

$$\begin{aligned}\Gamma_V^{\alpha\beta\mu}(q,\bar{q},P) = {} & f_1^V (q-\bar{q})^\mu g^{\alpha\beta} - \frac{f_2^V}{m_W^2}(q-\bar{q})^\mu P^\alpha P^\beta + f_3^V\left(P^\alpha g^{\mu\beta} - P^\beta g^{\mu\alpha}\right) \\ & + i f_4^V\left(P^\alpha g^{\mu\beta} + P^\beta g^{\mu\alpha}\right) + i f_5^V \varepsilon^{\mu\alpha\beta\rho}(q-\bar{q})_\rho \\ & - f_6^V \varepsilon^{\mu\alpha\beta\rho} P_\rho - \frac{f_7^V}{m_W^2}(q-\bar{q})^\mu \varepsilon^{\alpha\beta\rho\sigma} P_\rho (q-\bar{q})_\sigma,\end{aligned} \tag{2.4}$$

for V = γ, Z. Here all the form factors f_i^V are dimensionless functions of P^2. The expression (2.4) agrees with the one adopted by Gaemers and Gounaris [12] apart from their form factors f_8^V and f_9^V which are actually redundant. This fact is shown in appendix A.

* If the W's are off mass-shell, additional derivatives $\Box^l W_\mu^+, \Box^m W_\mu$ (l, m integer) complete all possible operators. The spin-0 part can still be neglected in so far as the W's couple to massless fermion pairs.

** It should be kept in mind that the choice of the two dimension-6 operators in (2.1) is not unique. Actually, the operators which correspond to the vertex function (2.4) represent another choice. However, this nonuniqueness merely amounts to a different P^2 dependence of the form factors.

It is straightforward to calculate the contribution of the lowest-dimensional operators (2.1) to the seven form factors. We find,

$$f_1^V = g_1^V + \frac{s}{2m_W^2}\lambda_V,$$

$$f_2^V = \lambda_V,$$

$$f_3^V = g_1^V + \kappa_V + \lambda_V,$$

$$f_i^V = g_i^V \qquad \text{for } i = 4,5,$$

$$f_6^V = \tilde{\kappa}_V - \tilde{\lambda}_V,$$

$$f_7^V = -\tfrac{1}{2}\tilde{\lambda}_V. \tag{2.5}$$

Contributions from the higher dimensional operators provide the P^2 dependence of the form factors. (For instance, if we restrict ourselves to the corresponding operators of dimension 6 or less, the form factors f_2 and f_7 are constants, and the others are linear functions of P^2.) Hermiticity requires that the f_i^V's should be real for $P^2 < 0$. However, the form factors may have imaginary parts above threshold, which we will discuss shortly.

Without losing generality, we can fix the overall coupling constants g_{WWV}. We choose for convenience

$$g_{WW\gamma} = -e, \qquad g_{WWZ} = -e\cot\theta_w, \tag{2.6}$$

where e denotes the positron charge and θ_w is the weak mixing angle of the standard model.

For the photon couplings ($V = \gamma$), the first term in eq. (2.1) (with $g_1^\gamma = 1$ determining the charge of the W) is the so-called "minimal" coupling term, and the second coefficient κ_γ is conventionally called the "anomalous" magnetic moment of the W [43]. This term and the third coefficient [3,5,44] λ_γ are related to the magnetic moment μ_W and the electric quadrupole moment Q_W of the W^+ by

$$\mu_W = \frac{e}{2m_W}(1 + \kappa_\gamma + \lambda_\gamma), \tag{2.7a}$$

$$Q_W = -\frac{e}{m_W^2}(\kappa_\gamma - \lambda_\gamma). \tag{2.7b}$$

These first three couplings respect the discrete symmetries P, C, and T separately

with the following definitions:

$$\mathscr{C}W_\mu\mathscr{C}^{-1} = -W_\mu^\dagger, \qquad \mathscr{C}V_\mu\mathscr{C}^{-1} = -V_\mu,$$

$$\mathscr{P}B_\mu(x,t)\mathscr{P}^{-1} = B^\mu(-x,t),$$

$$\mathscr{T}B_\mu(x,t)\mathscr{T}^{-1} = B^\mu(x,-t), \tag{2.8}$$

for $B^\mu = W^\mu, V^\mu$. The symmetry properties are most easily established by applying the above transformation to the effective lagrangian (2.1).

Two of the parity-violating couplings $\tilde{\kappa}_\gamma$ and $\tilde{\lambda}_\gamma$ respect charge conjugation invariance. They are related to the electric dipole moment d_W and the magnetic quadrupole moment $\tilde{Q}_W$ of W^+ by

$$d_W = \frac{e}{2m_W}\left(\tilde{\kappa}_\gamma + \tilde{\lambda}_\gamma\right), \tag{2.9a}$$

$$\tilde{Q}_W = -\frac{e}{m_W^2}\left(\tilde{\kappa}_\gamma - \tilde{\lambda}_\gamma\right). \tag{2.9b}$$

Finally, the other two couplings g_4^γ and g_5^γ in eq. (2.1) violate charge conjugation symmetry. However, the former coupling respects parity whereas the latter is CP invariant. These properties of the form factors f_i^V under discrete transformations are summarized in table 1.

If the underlying dynamics respects some of the above discrete symmetries, the corresponding form factors which are odd under these transformations would be identically zero. To be completely general, however, one should retain all these form factors in the WWγ or WWZ coupling.

For the photon the effective lagrangian (2.1) is not gauge invariant when g_4^γ or g_5^γ is nonvanishing. However, this can be cured by considering higher-dimensional operators. At the level of the vertex function (2.4) we may modify the f_4^γ and f_5^γ terms to

$$if_4^\gamma\left(P^\alpha g^{\mu\beta} + P^\beta g^{\mu\alpha} - 2P^\mu P^\alpha P^\beta/P^2\right)$$
$$+ if_5^\gamma\left[\varepsilon^{\mu\alpha\beta\rho}(q-\bar{q})_\rho - P^\mu\varepsilon^{\alpha\beta\rho\sigma}P_\rho(q-\bar{q})_\sigma/P^2\right], \tag{2.10}$$

TABLE 1
Properties of the couplings f_i^V (V = γ, Z) under discrete transformations

i	1–3	4	5	6, 7
P	+	+	−	−
CP	+	−	+	−
C	+	−	−	+

without affecting the amplitudes for $e^+e^- \to W^+W^-$. Now the absence of a pole at $P^2 = 0$ implies that f_4^γ and f_5^γ should be proportional to $P^2 = s$. Another constraint arises because the W^+ charge is fixed ($g_1^\gamma = 1$ in eq. (2.5)). We thus obtain the following constraints on the WWγ couplings at $s = 0$

$$f_1^\gamma(s=0) = 1, \tag{2.11a}$$

$$f_i^\gamma(s=0) = 0 \qquad \text{for } i = 4,5. \tag{2.11b}$$

The imaginary parts of the form factors are essentially the absorptive part of the WWV vertex function. Such effects are proportional to small coupling constants in a weakly coupled theory such as the standard model. However, they can be substantial if the W boson sector is strongly interacting in the relevant region of s. Actually in such a situation, not only the WWV vertex we are parametrizing but also the amplitudes for the whole process $e^+e^- \to W^+W^-$ may be affected substantially by the strong interaction. In what follows we neglect this possibility and shall study mainly the case where all the form factors are approximately real. We shall return to this point in sect. 4 and see that such strong rescattering effects have distinctive experimental signatures.

In principle, there are some purely phenomenological constraints on the couplings in eq. (2.4) arising from the anomalous magnetic moment of charged leptons [45], the electric dipole moment of leptons and neutrons [46], and the so-called ρ parameter [47]. However, we shall largely ignore these constraints for the following reasons. First, the couplings which enter in these calculations have different kinematical configurations: $p_\gamma^2 \simeq 0$ in the first two cases and p_Z^2 or $p_W^2 \simeq 0$ in the last case. Second, even if one assumes constant form factors in the relevant regions, there is always a possibility of cancellation among different contributions which renders these bounds ineffective. Direct studies of W-pair production at high-energy experiments are in this sense quite complementary to these precision experiments at low energies. Although the interplay between high- and low-energy experimental constraints is important, the latter bounds by no means can replace the rôle of high-energy measurements.

Strong constraints on the s dependence of the form factors occur if the size of the W boson, Λ^{-1}, is much smaller than the scale one can probe, $(1/\sqrt{s})$. In such a case we can expand all the form factors around $s = 0$,

$$f_i^V(s) = f_i^V(0) + O(s/\Lambda^2), \tag{2.12}$$

and thus constraints like eqs. (2.11) become effective. Furthermore, naïve dimensional considerations tell us that all the dimension $d > 4$ operators should scale as Λ^{4-d}, which implies

$$f_i^\gamma(s) = O(s/\Lambda^2) \qquad \text{for } i = 2,4,5,7,$$

$$f_i^Z(s) = O(s/\Lambda^2) \qquad \text{for } i = 2,7. \tag{2.13}$$

It is often argued that the scale of compositeness may be of the order of 1 TeV or higher*. However, because of the ambiguity in defining Λ and also because of the high energies of LEP-II, $\sqrt{s} \sim 0.2$ TeV, it may not be completely safe to ignore the $O(s/\Lambda^2)$ terms**. In any case, in the energy region covered by LEP-II, we may take the form factors to be approximately constant

$$f_i^V(s) \sim f_i^V(4m_W^2).$$

Note, however, that these values of the form factors may be different from those at $s = 0$.

In the standard model, non-abelian gauge symmetry gives very strong constraints on the couplings of eq. (2.4):

$$f_1^V(s) = 1 + O(\alpha), \tag{2.14a}$$

$$f_2^V(s) = O(\alpha), \tag{2.14b}$$

$$f_3^V(s) = 2 + O(\alpha), \tag{2.14c}$$

for both $V = \gamma, Z$, while all other form factors which violate either P or C invariance are either $O(\alpha)$ or higher. (Actually they receive contributions only from fermion loops.) Notice that the s dependence appears only at order α and hence the standard-model constraint (2.14a) is much stronger than the condition (2.11a). The constraints (2.14) can also be written as

$$\kappa_V = 1 + O(\alpha), \tag{2.15a}$$

$$\lambda_V = O(\alpha), \tag{2.15b}$$

for $V = \gamma, Z$.

3. Helicity amplitudes for $e^+e^- \to W^+W^-$

In this section we give polarization amplitudes for the process

$$e^-(k,\sigma) + e^+(\bar{k},\bar{\sigma}) \to W^-(q,\lambda) + W^+(\bar{q},\bar{\lambda}), \tag{3.1}$$

as depicted in fig. 3, with the general three-vector-boson couplings (2.4). (The

* For a recent review on the compositeness scale, see e.g., ref. [48].

** We have chosen the seven operators to give the most general spin structure. From the viewpoint of dimensional counting, it may be more consistent to choose $f_2 = f_7 = 0$ or give extra linear s dependence to the other five form factors: $f_i(s) = f_i(0) + f_i' \cdot s$. However, we are not interested in the energy dependence of the form factors (except for threshold behavior) because LEP-II will not cover a wide energy range. If one is to study higher-energy behavior of the reaction, one should take into account the effect of unitarity and final state interactions (ref. [49]).

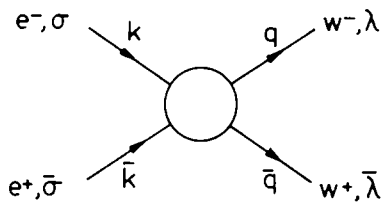

Fig. 3. Schematical view of the process $e^+e^- \to W^+W^-$. Indices σ, $\bar{\sigma}$, λ, and $\bar{\lambda}$ denote helicities.

four-momentum and the helicity of each particle are shown in parenthesis.) We discuss here only the amplitudes for on-shell W pair production; the more general case with off-shell W's is treated in appendix C.

Helicity amplitudes contain more information than the cross section for polarized W's. The relative phases of the amplitudes are important for the distribution of the final fermions because the interference of different W helicity states gives a nontrivial azimuthal-angle dependence. Furthermore, polarization of the initial e^+e^- beams can be taken into account in a straightforward manner

The helicity of a massive particle is not a relativistically invariant quantity. It is invariant only for rotations or boosts along the particle's momentum, as long as the momentum does not change its sign. In this paper we define the helicities of the W in the e^+e^- c.m. frame, which is the natural frame of the problem.

It is well known that a longitudinally polarized vector boson leads to a possible bad high-energy behavior. If we take the W boson momentum in the positive z direction

$$p_W = (E_W, 0, 0, p_W), \tag{3.2}$$

the transverse (helicity-± 1) polarization vectors are given by

$$\varepsilon_{(\pm 1)} = \sqrt{\tfrac{1}{2}}\,(0, \mp 1, -i, 0), \tag{3.3a}$$

whereas the longitudinal (helicity-0) vector is

$$\begin{aligned}\varepsilon_{(0)} &= m_W^{-1}(p_W, 0, 0, E_W) \\ &= (\gamma\beta, 0, 0, \gamma),\end{aligned} \tag{3.3b}$$

where $\gamma = E_W/m_W$, $\beta = (1 - m_W^2/E_W^2)^{1/2}$. It is this γ factor that leads, with its extra power of energy, to a possible breakdown of unitarity at high energies. For example, if we restrict ourselves to dimension-4 interactions, the high-energy behavior of a tree amplitude is given by γ^N, where N is the number of longitudinal W's in the final state. (Note that the longitudinal part of the virtual Z does not contribute because it couples to a conserved electron current.) For dimension-6 interactions there are two extra factors of γ, and so on.

TABLE 2
Explicit form of the d functions needed

$$d^2_{1,2} = -d^2_{1,-2} = \tfrac{1}{2}(1+\cos\theta)\sin\theta$$
$$d^2_{1,-2} = -d^2_{-1,2} = -\tfrac{1}{2}(1-\cos\theta)\sin\theta$$
$$d^1_{1,1} = d^1_{-1,-1} = \tfrac{1}{2}(1+\cos\theta)$$
$$d^1_{1,-1} = d^1_{-1,1} = \tfrac{1}{2}(1-\cos\theta)$$
$$d^1_{1,0} = -d^1_{-1,0} = -\sqrt{\tfrac{1}{2}}\sin\theta$$

3.1. HELICITY AMPLITUDES

We have calculated the polarization amplitudes by using two different spinor calculus techniques. One [42] is a very straightforward and general method based on two-component spinors developed by two of us. The other [49] uses a non-covariant d-function representation of spinors and vectors, and is convenient for two-body reactions. Both methods give the same result. Our results also agree with the result of Gaemers and Gounaris [12] who used a rectangular basis for W's.

In this section we present the results* in a compact form [49] using the helicity basis for W's. For convenience we extract some factors from the amplitude

$$\mathcal{M}_{\sigma\bar{\sigma};\lambda\bar{\lambda}}(\Theta) = \sqrt{2}\, e^2 \tilde{\mathcal{M}}_{\sigma\bar{\sigma};\lambda\bar{\lambda}}(\Theta)\, \varepsilon d^{J_0}_{\Delta\sigma,\Delta\lambda}(\Theta), \tag{3.4}$$

where $\varepsilon = \Delta\sigma(-1)^{\bar{\lambda}}$ is a sign factor, $\Delta\sigma = \frac{1}{2}(\sigma - \bar{\sigma})$, $\Delta\lambda = \lambda - \bar{\lambda}$, $J_0 = \max(|\Delta\sigma|, |\Delta\lambda|)$, and Θ denotes the scattering angle of W^- with respect to the e^- direction in the e^+e^- c.m. frame. Finally $d^{J_0}_{\Delta\sigma,\Delta\lambda}$ is the d function in the convention of Rose [50]. The explicit form of the d functions needed here is reproduced in table 2. Note that $\tilde{\mathcal{M}}$ is not a partial wave amplitude because it can still have a Θ dependence. Rather, J_0 is the minimum angular momentum of the system and the amplitude includes partial waves of $J = J_0, J_0+1, \ldots$.

Two of the three lowest-order diagrams, namely those with s-channel γ and Z exchange (fig. 1a, b), have only $J = 1$ partial wave because of angular momentum conservation. On the other hand, the diagram with t-channel ν exchange (fig. 1c) has all the partial waves with $J \geqslant J_0$. It is convenient to discuss the cases $J_0 = 1$ and 2 separately. (Since we are neglecting the electron mass, conservation of the electron chirality excludes the case $J_0 = 0$, because $\Delta\sigma$ is either 1 or -1.)

The case $J_0 = 2$ is simple. The above argument shows that only the ν exchange diagram contributes to this final state. Moreover, because $|\Delta\lambda| = 2$, the final W

* Our results can be obtained by evaluating the sum $\mathcal{M}^\nu + \mathcal{M}^\gamma + \mathcal{M}^Z$ presented in eqs. (C.11) and (C.12) in the e^+e^- c.m. frame where the electron beam direction is chosen as the z-axis and the W^- transverse momentum as the x-axis. The phase convention thus follows that of ref. [42]. The amplitudes in Jacob-Wick phase convention in the above frame can be obtained from eq. (3.4) by dropping the sign factor ε. Also, in this paper we normalize the fermion helicities to ± 1.

bosons are both transverse [$(\lambda\bar{\lambda}) = (+-)$ or $(-+)$]. Thus these amplitudes do not have a bad high-energy behavior:

$$\tilde{\mathcal{M}} = -\frac{\sqrt{2}}{\sin^2\theta_w}\frac{1}{1+\beta^2-2\beta\cos\Theta}\delta_{\Delta\sigma,-1} \qquad (\Delta\lambda = \pm 2). \tag{3.5}$$

The other seven final helicity combinations give $J_0 = 1$. Five of them have at least one longitudinal W, which could give a possible divergent behavior at high energies. We write the amplitude as a sum of three contributions

$$\tilde{\mathcal{M}} = \tilde{\mathcal{M}}^\gamma + \tilde{\mathcal{M}}^Z + \tilde{\mathcal{M}}^\nu \qquad (\Delta\lambda \leqslant 1), \tag{3.6}$$

where

$$\tilde{\mathcal{M}}^\gamma = -\beta\delta_{|\Delta\sigma|,1}A^\gamma_{\lambda\bar{\lambda}}, \tag{3.7a}$$

$$\tilde{\mathcal{M}}^Z = \beta\left[\delta_{|\Delta\sigma|,1} - \frac{1}{2\sin^2\theta_w}\delta_{\Delta\sigma,-1}\right]\frac{s}{s-m_Z^2}A^Z_{\lambda\bar{\lambda}}, \tag{3.7b}$$

$$\tilde{\mathcal{M}}^\nu = \frac{1}{2\sin^2\theta_w\beta}\delta_{\Delta\sigma,-1}\left[B_{\lambda\bar{\lambda}} - \frac{1}{1+\beta^2-2\beta\cos\Theta}C_{\lambda\bar{\lambda}}\right]. \tag{3.7c}$$

The coefficients A, B, C for the standard model are shown in table 3. For the general WWV coupling the A coefficients are tabulated in table 4.

3.2. STANDARD MODEL

Using eq. (3.7) one can readily appreciate the structure of the gauge-theory cancellation in the standard model, which provides a good high-energy behavior. First note that the bad high-energy behavior is confined to the $J = 1$ partial wave, because the second term of the ν exchange contribution (3.7c) is regular at high energies (see the coefficient C in table 3). This is in fact necessary for the

TABLE 3
Coefficients $A^\gamma_{\lambda\bar{\lambda}} = A^Z_{\lambda\bar{\lambda}}$, $B_{\lambda\bar{\lambda}}$, and $C_{\lambda\bar{\lambda}}$ in (3.7) for the standard model

$\Delta\lambda$	$(\lambda\bar{\lambda})$	$A^{\gamma,Z}_{\lambda\bar{\lambda}}$	$B_{\lambda\bar{\lambda}}$	$C_{\lambda\bar{\lambda}}$
1	$(+0),(0-)$	2γ	2γ	$2(1+\beta)/\gamma$
-1	$(0+),(-0)$	2γ	2γ	$2(1-\beta)/\gamma$
0	$(++),(--)$	1	1	$1/\gamma^2$
0	(00)	$2\gamma^2+1$	$2\gamma^2$	$2/\gamma^2$

$\beta = (1-4m_W^2/s)^{1/2}$ and $\gamma = \sqrt{s}/2m_W$.

TABLE 4
Coefficients $A^V_{\lambda\bar{\lambda}}$ for the general coupling (2.4)

$\Delta\lambda$	$(\lambda\bar{\lambda})$	$A^V_{\lambda\bar{\lambda}}$
1	$(+0)$	$\gamma(f_3^V - if_4^V + \beta f_5^V + i\beta^{-1}f_6^V)$
1	$(0-)$	$\gamma(f_3^V + if_4^V + \beta f_5^V - i\beta^{-1}f_6^V)$
−1	$(0+)$	$\gamma(f_3^V + if_4^V - \beta f_5^V + i\beta^{-1}f_6^V)$
−1	(-0)	$\gamma(f_3^V - if_4^V - \beta f_5^V - i\beta^{-1}f_6^V)$
0	$(++)$	$f_1^V + i\beta^{-1}f_6^V + 4i\gamma^2\beta f_7^V$
0	$(--)$	$f_1^V - i\beta^{-1}f_6^V - 4i\gamma^2\beta f_7^V$
0	(00)	$\gamma^2[-(1+\beta^2)f_1^V + 4\gamma^2\beta^2 f_2^V + 2f_3^V]$

The last coefficient A^V_{00} can be alternatively written as $g_1^V + 2\gamma^2\kappa_V$.

cancellation, because the γ and Z exchange diagrams have $J = 1$ only. So one need only concentrate on the A and B contribution.

Some of the coefficients A and B (table 3) are proportional to γ or γ^2 as expected from longitudinal W counting. However, all the divergent parts are common to all three diagrams. At high energies ($\gamma \to \infty$, $\beta \to 1$), we have

$$A^\gamma_{\lambda\bar{\lambda}} = A^Z_{\lambda\bar{\lambda}} = B_{\lambda\bar{\lambda}}, \tag{3.8}$$

up to an O(1) term. The Z contribution (3.7b) is separated into two terms. The first term conserves parity (thus "electromagnetic" component), and is canceled by the γ-exchange contribution at high energies. The second term in (3.7b), which exists for the left-handed electron only (thus weak isovector or "W^0" component) is canceled by the ν-exchange B term.

Because the cancellation reduces the power of γ by 2, the amplitudes for one longitudinal and one transverse W pair ($\Delta\lambda = \pm 1$) go down as γ^{-1} at high energies. From table 3 one also readily sees that the amplitudes for two of the $\Delta\lambda = 0$ states ($(\lambda\bar{\lambda}) = (++)$ and $(--)$) are suppressed by γ^{-2}. Thus only three of the nine helicity combinations, namely $(+-)$, $(-+)$, and (00), survive at high energies for finite scattering angle Θ.

These three amplitudes do not contribute to the cross section equally. The $\Delta\lambda = -2$ $(-+)$ amplitude (3.5) dominates over the other two at high energies because of the t-channel pole factor $1/(1+\beta^2-2\beta\cos\Theta)$ which peaks at $\cos\Theta = 1$ with a γ^4 enhancement. (In practice the peak in the $(-+)$ amplitude appears slightly below $\cos\Theta = 1$ because the function $d^2_{-1,-2}$ is proportional to $\sin\Theta$ and vanishes at $|\cos\Theta| = 1$.) A kinematic zero kills the t-channel pole for the $(+-)$ amplitude. For the (00) final state the pole term is suppressed by a dynamical γ^{-2} factor in the C coefficient and further softened by a kinematical $\sin\Theta$ factor.

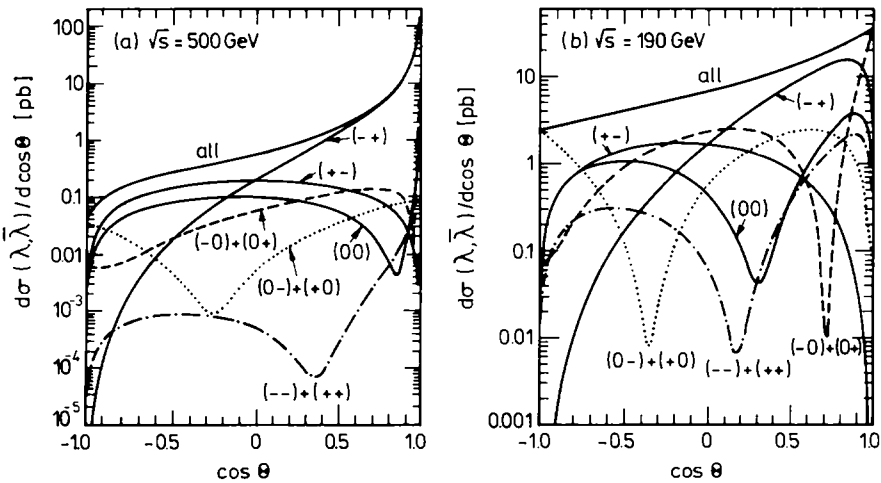

Fig. 4. Angular distribution $d\sigma(\lambda, \bar{\lambda})/d\cos\Theta$ of polarized W^-W^+ production in e^+e^- annihilation at (a) $\sqrt{s} = 500$ GeV and (b) 190 GeV, averaged over initial lepton polarizations. Shown in parentheses are W^- and W^+ helicities in the e^+e^- c.m. frame.

Moreover, even at large angles, the (00) amplitude happens to be numerically smaller than the transverse amplitudes. Thus the dominant final state is purely transverse and there is a strong forward peaking. These characteristics can be seen from fig. 4a, where the cross section for each final helicity state at $\sqrt{s} = 500$ GeV is shown.

Even at LEP-II energies ($\sqrt{s} \lesssim 200$ GeV), these tendencies already appear. At $\sqrt{s} = 190$ GeV, the ratio of transverse to longitudinal W's is about 3 : 1. The cross section for polarized W's is plotted in fig. 4b for this energy. The $\Delta\lambda = -1$ states have an appreciable contribution to the cross section at this energy, which in fact is the second largest. However, the dominance of the $\Delta\lambda = -2$ state already holds.

At threshold, the behavior of the cross section is quite restricted. Since no orbital angular momentum is allowed between the final W's, the total spin is equal to total angular momentum. It can take the values 0, 1, 2. However, it turns out that only $J = 2$ is allowed under quite general conditions, as we shall explain below. In this case all helicity amplitudes at threshold are related by Clebsch-Gordan coefficients irrespective of detailed dynamics. This fact may provide an interesting opportunity to uncover exotic interactions. A chirality-nonconserving interaction of electrons (scalar or heavy lepton exchange [16], for example) gives a $J = 0$ final state, and *CP*-violating three-boson interaction can give $J = 1$. (The latter possibility will be discussed later in this section.)

The proof of the above assertion is rather straightforward. Among the three possible angular momenta $J = 0, 1, 2$, $J = 0$ is forbidden by electron chirality conservation because the initial state can have only $J \geqslant 1$ [up to $O(m_e)$]. *CP*

invariance forbids $J=1$ because the initial e^+e^- state should have $CP=+1$ ($J^{PC}=1^{++}/1^{--}, 2^{++}/2^{--},\ldots$) and the final W^+W^- state should have $J^{PC}=0^{++}$, 1^{+-}, or 2^{++}. For $J=2$ there is no selection rule to forbid the reaction. In fact, in the standard model, the process receives a contribution from ν exchange.

Finally we note that for polarized beams containing e^-_R and/or e^+_L, only the pure longitudinal final state (00) remains at high energies because ν exchange does not contribute. However, the cross section for this helicity combination is only $\sim 10^{-2}$ of the unpolarized cross section.

3.3. GENERAL THREE-BOSON COUPLINGS

For general couplings (table 4), the cancellation detailed above no longer occurs. The worst case exhibits a γ^4 behavior. Of course, form factors and/or higher order contributions should provide the necessary damping in this case to guarantee eventually that partial-wave unitarity is not violated.

Even for general couplings, however, the cancellation in the "electromagnetic" part takes place if $f_i^\gamma = f_i^Z$ is satisfied. Numerically, more than 70% of the γ exchange amplitude (3.7a) is canceled by the "electromagnetic" term of the Z exchange (3.7b) already at $\sqrt{s}=200$ GeV. Violation of this cancellation by $f_i^\gamma \neq f_i^Z$ can be seen most directly in the $\Delta\sigma=1$ channel. Separation of this channel from the dominant $\Delta\sigma=-1$ channel can be achieved by measuring the azimuthal-angle dependence when the beams are transversely polarized, or by using longitudinally polarized beam(s) (see subsect. 5.4 below).

For the "weak isovector" part, the cancellation between the Z- and ν-exchange contributions (B terms only) is numerically less significant (40% at $\sqrt{s}=200$ GeV) because of the difference in the threshold behavior. Indeed, the ν-exchange amplitude dominates near threshold* (S wave) whereas the s-channel exchange contribution is suppressed by at least a factor of β (P wave). Hence, in the threshold region, the reaction $e^+e^- \to W^+W^-$ is not very sensitive to the three-vector-boson coupling.

There is an exception to the above conclusion which was already noted in the preceding subsection. We see from table 4 that if the CP-violating coupling f_6^V is nonzero, the γ- and Z-exchange amplitudes have S-wave behavior. Tests of CP (see subsect. 5.2) near the threshold can thus constrain f_6^V rather independently of the other couplings.

Because the standard model prediction is far below the unitarity limit, the cross section will become very sensitive to anomalous couplings at high energies ($\gamma \gg 1$) through the violation of the gauge-theory cancellation. Unfortunately, the energy range available at LEP-II is not high enough ($\gamma^2 \simeq 1.5$ at $\sqrt{s}=200$ GeV) and we need a detailed study to constrain these couplings, as will be discussed in the next two sections.

* The β^{-1} factor in (3.7c) is spurious and the $\beta \to 0$ limit is finite.

3.4. SYMMETRY PROPERTIES

Before closing this section, we remark on some general restrictions to the full amplitudes (3.4). (Corresponding details for the cross section appear in subsect. 4.3.) It is easy to see that if all the form factors f_i^V are real the following equation holds:

$$\tilde{\mathcal{M}}_{\sigma\bar{\sigma};\lambda\bar{\lambda}} = \tilde{\mathcal{M}}^*_{-\bar{\sigma},-\sigma;-\bar{\lambda},-\lambda}. \tag{3.9}$$

This is a consequence of *CPT* invariance *and* the absence of absorptive parts. Hence violation of this relation immediately indicates substantial rescattering effects. This fact can be seen as follows. *CPT* invariance gives the following relation between scattering amplitudes (with appropriate phase convention)

$$T_{fi} = T_{\hat{i}\hat{f}}, \tag{3.10}$$

where $\hat{i}(\hat{f})$ denotes the *CPT* conjugate state of a state $i(f)$. This relation is not immediately useful for our purpose, because it connects the amplitude for the reaction $e^+e^- \to W^+W^-$ to that for $W^+W^- \to e^+e^-$. However we find

$$\begin{aligned} T_{fi} - T^*_{\hat{f}\hat{i}} &= T_{fi} - T^\dagger_{\hat{i}\hat{f}} \\ &= T_{fi} - T^\dagger_{fi}. \end{aligned} \tag{3.11}$$

Here we have used *CPT* invariance for the second equality. If the T matrix is hermitian, we have

$$T_{fi} = T^*_{\hat{f}\hat{i}}. \tag{3.12}$$

This is actually the case in the Born approximation. Unitarity tells us that $T - T^\dagger$ is the absorptive part which arises from rescattering effects. Thus in a weakly coupled theory eq. (3.12) holds to a good approximation. When applied to the reaction $e^+e^- \to W^+W^-$, it gives eq. (3.9).

CP invariance leads to the relation

$$\tilde{\mathcal{M}}_{\sigma\bar{\sigma};\lambda\bar{\lambda}} = \tilde{\mathcal{M}}_{-\bar{\sigma},-\sigma;\bar{\lambda},-\lambda}, \tag{3.13}$$

which can be directly used as a test of *CP* conservation. This test does not assume the absence of absorptive parts*.

* It should be noted that the relations (3.9) and (3.13) are simpler than their appearance. Actually they connect the same initial state for nonvanishing amplitudes: $(\sigma\bar{\sigma}) = (\mp\,\mp) = (\cdot\cdot\bar{\sigma}, -\sigma)$. As for the final state, they relate states with same $\Delta\lambda$:

$$\begin{aligned} \Delta\lambda = +1: &\quad (\lambda\bar{\lambda}) = (+0) \leftrightarrow (0-), \\ 0: &\quad (++) \leftrightarrow (--), \\ -1: &\quad (0+) \leftrightarrow (-0). \end{aligned}$$

It is also possible to write down similar relations derivable from C or P invariance. However, they are not very useful since the ν-exchange contribution already violates C and P maximally. It is not easy to obtain simple relationships for the amplitudes which signal C or P nonconservation in the vector boson sector*.

4. Angular correlations for final state fermions

In this section we present the most general angular distributions of the decay products in the process

$$\begin{aligned} &e^-(k,\sigma)+e^+(\bar{k},\bar{\sigma}) \to W^-(q,\lambda)+W^+(\bar{q},\bar{\lambda}), \\ &W^-(q,\lambda) \to f_1(p_1,\sigma_1)+\bar{f}_2(p_2,\sigma_2), \\ &W^+(\bar{q},\bar{\lambda}) \to f_3(p_3,\sigma_3)+\bar{f}_4(p_4,\sigma_4), \end{aligned} \tag{4.1}$$

with massless fermions. As the material in this section is rather technical, the reader who is only interested in the results may proceed to sect. 5.

Since we understand the decay interactions well, we can extract explicitly the dependence of the cross section on final fermion angles. The fact that the W has spin one restricts the possible form of the angular dependence to a finite but large number of terms (actually 81). The coefficient of each term can be written in terms of the production density matrix, which may be obtained from the polarization amplitudes presented in sect. 3 or appendix C.

4.1. DERIVATION

The full amplitude can be expressed as follows (see fig. 5):

$$\begin{aligned} \mathcal{M}(k,\sigma;\bar{k},\bar{\sigma};p_i,\sigma_i) = D_W(q^2)D_W(\bar{q}^2)\sum_{\lambda}\sum_{\bar{\lambda}}\mathcal{M}_1(k,\sigma;\bar{k},\bar{\sigma};q,\lambda;\bar{q},\bar{\lambda}) \\ \times\mathcal{M}_2(q,\lambda;p_1,\sigma_1;p_2,\sigma_2)\mathcal{M}_3(\bar{q},\bar{\lambda};p_3,\sigma_3;p_4,\sigma_4), \end{aligned} \tag{4.2}$$

* For the three-boson coefficient $A^V_{\lambda\bar{\lambda}}$, we can write down the requirement from P, C, and CP invariance as follows:

$$P: \quad A^V_{\lambda\bar{\lambda}} = A^V_{-\lambda,-\bar{\lambda}},$$

$$C: \quad A^V_{\lambda\bar{\lambda}} = A^V_{\bar{\lambda}\lambda},$$

$$CP: \quad A^V_{\lambda\bar{\lambda}} = A^V_{\bar{\lambda},\lambda}.$$

The first two equations relate final states with opposite $\Delta\lambda$, while the last one relates those with the same $\Delta\lambda$.

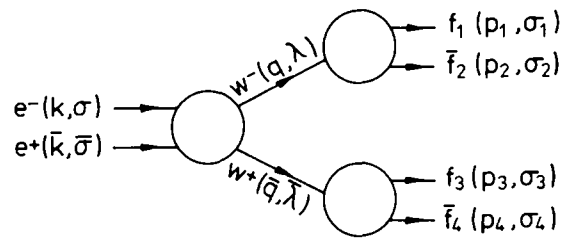

Fig. 5. Schematical view of the process $e^+e^- \to (W^- \to f_1\bar{f}_2) + (W^+ \to f_3\bar{f}_4)$. Shown in parentheses are four-momentum and helicity of the particles.

with the Breit-Wigner propagator factor for W bosons:

$$D_W(q^2) = \left(q^2 - m_W^2 + im_W\Gamma_W\right)^{-1}. \tag{4.3}$$

Here the summations over intermediate W polarizations can either be done in the Cartesian basis $\lambda, \bar{\lambda} = 1,2,3$ or in the helicity basis $\lambda, \bar{\lambda} = \pm, 0$. The former basis is convenient for the numerical evaluation of the amplitude (see appendix C), whereas the latter, which we take here, is more suited for theoretical considerations.

The production amplitude $\mathcal{M}_1$ is a sum of three contributions which are given in eqs. (C.11) and (C.12). Its explicit form in the e^+e^- c.m. frame for on-shell W's has been presented in sect. 3.

In the massless fermion limit (see eq. (C.19)), the W^- decay amplitude $\mathcal{M}_2$, as evaluated in appendix C (see eq. (C.16)), simplifies to give

$$\mathcal{M}_2 = eg_-^{Wf_1f_2} C\delta_{\sigma_1,-}\delta_{\sigma_2,+}2\sqrt{p_1^0p_2^0}\,S(p_1,\varepsilon(q,\lambda),p_2)^-{}_-. \tag{4.4}$$

Here $g_-^{Wf_1f_2}$ is the standard V − A coupling (C.15). The effective color factor C is 1 for leptons and $\sqrt{3}$ for quarks. The corresponding W^- decay amplitude $\mathcal{M}_3$ is obtained from (4.4) by the replacement $(1,2,q,\lambda) \to (3,4,\bar{q},\bar{\lambda})$. The spinorial string S (see eq. (C.7) for its definition) can be explicitly expressed in a given Lorentz frame.

In the c.m. frame of the colliding beams, we choose the W momentum direction as the z-axis and the $\boldsymbol{k}(e^-) \times \boldsymbol{q}(W^-)$ direction as the y-axis; the scattering $e^-e \to W^+W^-$ takes place in the x-z plane (see fig. 6). The production amplitude $\mathcal{M}_1$ is then a function of the scattering angle Θ between e^- and W^- momentum directions in this frame, as explicitly shown in the previous section. The decay amplitudes $\mathcal{M}_2$ and $\mathcal{M}_3$ are most simply expressed in the W and W^+ rest frame, respectively. We define each of these frames by a boost of the above e^+e^- c.m. frame along the z-axis.

In the W^- rest frame, we parametrize f_1 and $\bar{f}_2$ four-momenta as

$$p_1^\mu = \tfrac{1}{2}\sqrt{q^2}\,(1, \sin\theta\cos\phi, \sin\theta\sin\phi, \cos\theta),$$
$$p_2^\mu = \tfrac{1}{2}\sqrt{q^2}\,(1, -\sin\theta\cos\phi, -\sin\theta\sin\phi, -\cos\theta), \tag{4.5}$$

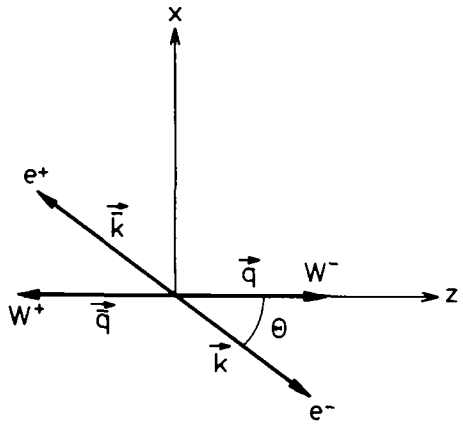

Fig. 6. The coordinate system in the colliding e^+e^- c.m. frame. The y-axis is chosen along the $\boldsymbol{k}(e^-) \times \boldsymbol{q}(W^-)$ direction and is pointing towards the observer. The coordinate systems in the W^- and W^+ rest frames are obtained from it by boosts along the z-axis.

and in the W^+ rest frame, we choose the antiparticle ($\bar{f}_4$) angles as $\bar{\theta}$ and $\bar{\phi}$,

$$p_3^\mu = \tfrac{1}{2}\sqrt{\bar{q}^2}\,(1, -\sin\bar{\theta}\cos\bar{\phi}, -\sin\bar{\theta}\sin\bar{\phi}, -\cos\bar{\theta}),$$

$$p_4^\mu = \tfrac{1}{2}\sqrt{\bar{q}^2}\,(1, \sin\bar{\theta}\cos\bar{\phi}, \sin\bar{\theta}\sin\bar{\phi}, \cos\bar{\theta}). \tag{4.6}$$

In this convention the angles of the charged lepton or the d-type quark are chosen as (θ, ϕ) in W^- decays and $(\bar{\theta}, \bar{\phi})$ in W^+ decays.

It is a straightforward exercise to evaluate the spinorial string S in (4.4) in these two frames. One finds

$$\mathcal{M}_2 = e g_-^{Wf_1f_2} C\sqrt{q^2}\,\delta_{\sigma_1,-}\delta_{\sigma_2,+} l_\lambda, \tag{4.7a}$$

$$\mathcal{M}_3 = -e g_-^{Wf_3f_4} \bar{C}\sqrt{\bar{q}^2}\,\delta_{\sigma_3,-}\delta_{\sigma_4,+} \bar{l}_{\bar{\lambda}}, \tag{4.7b}$$

where

$$(l_-, l_0, l_+) = (d_+ e^{-i\phi}, -d_0, d_- e^{i\phi}), \tag{4.8a}$$

$$(\bar{l}_-, \bar{l}_0, \bar{l}_+) = (\bar{d}_+ e^{i\bar{\phi}}, -\bar{d}_0, \bar{d}_- e^{-i\bar{\phi}}), \tag{4.8b}$$

with

$$\overset{(-)}{d}_\pm = \sqrt{\tfrac{1}{2}}\left(1 \pm \cos\overset{(-)}{\theta}\right), \qquad \overset{(-)}{d}_0 = \sin\overset{(-)}{\theta}. \tag{4.9}$$

Here C and $\bar{C}$ denote the effective color factors (1 or $\sqrt{3}$) for the corresponding W^- and W^+ decay processes.

4.2. CROSS SECTION FORMULAS

It is now straightforward to obtain the polarization-summed squared matrix elements

$$\sum|\mathcal{M}|^2 \equiv \sum_{\sigma}\sum_{\bar\sigma}\sum_{\sigma_1}\sum_{\sigma_2}\sum_{\sigma_3}\sum_{\sigma_4}\left|\mathcal{M}(k,\sigma;\bar k,\bar\sigma;p_i,\sigma_i)\right|^2$$

$$= e^4\left|g_-^{Wf_1f_2}g_-^{Wf_3f_4}\right|^2 C^2\bar C^2 q^2\bar q^2\left|D_W(q^2)D_W(\bar q^2)\right|^2 \mathcal{P}^{\lambda\bar\lambda}_{\lambda'\bar\lambda'}\mathcal{D}^{\lambda}_{\lambda'}\bar{\mathcal{D}}^{\bar\lambda}_{\bar\lambda}. \quad (4.10)$$

Here, and in the following, summation over repeated indices $(\lambda, \lambda', \bar\lambda, \bar\lambda') = \pm, 0$ is implied. The production tensor reads

$$\mathcal{P}^{\lambda\bar\lambda}_{\lambda'\bar\lambda'} = \sum_{\sigma}\sum_{\bar\sigma}\mathcal{M}_1(\sigma,\bar\sigma,\lambda,\bar\lambda;\Theta)\mathcal{M}_1^*(\sigma,\bar\sigma,\lambda',\bar\lambda';\Theta), \quad (4.11)$$

and the decay tensors are

$$\mathcal{D}^{\lambda}_{\lambda'} = l_\lambda l^*_{\lambda'}, \quad (4.12a)$$

$$\bar{\mathcal{D}}^{\bar\lambda}_{\bar\lambda'} = \bar l_{\bar\lambda}\bar l^*_{\bar\lambda'}. \quad (4.12b)$$

Eq. (4.10) gives the general structure of the polarization-summed squared matrix element for the process (4.1) with pure V − A couplings of the W to massless fermions. After integration over the virtual W mass squared, q^2 and $\bar q^2$, the differential cross section can be expressed as (in the narrow width approximation)

$$\frac{d\sigma}{d\cos\Theta\, d\cos\theta\, d\phi\, d\cos\bar\theta\, d\bar\phi} = \frac{9\beta}{8192\pi^3 s}B(W\to f_1\bar f_2)B(W\to f_3\bar f_4)\mathcal{P}^{\lambda\bar\lambda}_{\lambda'\bar\lambda'}\mathcal{D}^{\lambda}_{\lambda'}\bar{\mathcal{D}}^{\bar\lambda}_{\bar\lambda'}, \quad (4.13)$$

where $\beta = (1 - 4m_W^2/s)^{1/2}$. By integrating over W^+ decays, we obtain the inclusive $W^- \to f_1\bar f_2$ decay distribution

$$\frac{d\sigma}{d\cos\Theta\, d\cos\theta\, d\phi} = \frac{3\beta}{1024\pi^2 s}B(W\to f_1\bar f_2)\mathcal{P}^{\lambda\bar\lambda}_{\lambda'\bar\lambda}\mathcal{D}^{\lambda}_{\lambda'}, \quad (4.14a)$$

and alternatively we obtain the $W^+ \to f_3\bar f_4$ decay distribution as

$$\frac{d\sigma}{d\cos\Theta\, d\cos\bar\theta\, d\bar\phi} = \frac{3\beta}{1024\pi^2 s}B(W\to f_3\bar f_4)\mathcal{P}^{\lambda\bar\lambda}_{\lambda'\bar\lambda}\bar{\mathcal{D}}^{\bar\lambda}_{\bar\lambda'}. \quad (4.14b)$$

By further integrating out all the decay fermion angles, we simply get the differential cross section for the process $e^+e^- \to W^+W^-$:

$$\frac{d\sigma}{d\cos\Theta} = \frac{\beta}{128\pi s}\mathcal{P}^{\lambda\bar\lambda}_{\lambda\bar\lambda}. \quad (4.15)$$

By comparing eqs. (4.13)–(4.15), one can appreciate the additional information on the W^+W^- production amplitudes contained in decay fermion angular distributions.

It is useful to isolate explicitly the azimuthal-angle dependence in eq. (4.13). One finds

$$\begin{aligned}\mathscr{P}^{\lambda\bar{\lambda}}_{\lambda'\bar{\lambda}'}\mathscr{D}^{\lambda}_{\lambda'}\bar{\mathscr{D}}^{\bar{\lambda}}_{\bar{\lambda}'} = A + \{2\,\mathrm{Re}[&B\cos\phi + \bar{B}\cos\bar{\phi} + C\cos 2\phi + \bar{C}\cos 2\bar{\phi} \\ &+ D_{\pm}\cos(\phi \pm \bar{\phi}) + E_{\pm}\cos(2\phi \pm \bar{\phi}) + \bar{E}_{\pm}\cos(\phi \pm 2\bar{\phi}) \\ &+ G_{\pm}\cos(2\phi \pm 2\bar{\phi})] + (\mathrm{Re} \to \mathrm{Im}, \cos \to \sin)\}, \end{aligned} \tag{4.16}$$

where a shorthand notation such as $D_{\pm}\cos(\phi \pm \bar{\phi})$ for $D_{+}\cos(\phi + \bar{\phi}) + D_{-}\cos(\phi - \bar{\phi})$ is used, and

$$A = \mathscr{P}^{\lambda\bar{\lambda}}_{\lambda\bar{\lambda}} d^2_{-\lambda} d^2_{-\bar{\lambda}}, \tag{4.17a}$$

$$B = \left(\mathscr{P}^{-\bar{\lambda}}_{0\bar{\lambda}} d_{+} + \mathscr{P}^{0\bar{\lambda}}_{+\bar{\lambda}} d_{-}\right)\left(-d_0 \bar{d}^2_{-\bar{\lambda}}\right), \tag{4.17b}$$

$$\bar{B} = \left(\mathscr{P}^{\lambda +}_{\lambda 0} \bar{d}_{-} + \mathscr{P}^{\lambda 0}_{\lambda -} \bar{d}_{+}\right)\left(-\bar{d}_0 d^2_{-\lambda}\right), \tag{4.17c}$$

$$C = \mathscr{P}^{-\bar{\lambda}}_{+\bar{\lambda}} d_{+} d_{-} \bar{d}^2_{-\bar{\lambda}}, \tag{4.17d}$$

$$\bar{C} = \mathscr{P}^{\lambda +}_{\lambda -} \bar{d}_{+} \bar{d}_{-} d^2_{-\lambda}, \tag{4.17e}$$

$$D_{\pm} = \left[\left(\mathscr{P}^{-\pm}_{0\,0} \bar{d}_{\mp} + \mathscr{P}^{-\,0}_{0\,\mp} \bar{d}_{\pm}\right) d_{+} + \left(\mathscr{P}^{0\pm}_{+\,0} \bar{d}_{\mp} + \mathscr{P}^{0\,0}_{+\,\mp} \bar{d}_{\pm}\right) d_{-}\right] d_0 \bar{d}_0, \tag{4.17f}$$

$$E_{\pm} = \left(\mathscr{P}^{-\pm}_{+\,0} \bar{d}_{\mp} + \mathscr{P}^{-\,0}_{+\,\mp} \bar{d}_{\pm}\right)\left(-\bar{d}_0 d_{+} d_{-}\right), \tag{4.17g}$$

$$\bar{E}_{+} = \left(\mathscr{P}^{-\pm}_{0\,\mp} d_{+} + \mathscr{P}^{0\pm}_{+\,\mp} d_{-}\right)\left(-d_0 \bar{d}_{+} \bar{d}_{-}\right), \tag{4.17h}$$

$$G_{\pm} = \mathscr{P}^{-\pm}_{+\,\mp} d_{+} d_{-} \bar{d}_{+} \bar{d}_{-}. \tag{4.17i}$$

There are 25 independent azimuthal-angle distributions (including the constant piece A), as seen explicitly in (4.16). By taking into account the polar angle distributions in θ and $\bar{\theta}$ (see eq. (4.9)), one sees that there are nine independent distributions in A, 24 in B and $\bar{B}$ (counting both the real and imaginary parts), 12 in C and $\bar{C}$, 16 in $D_{\pm}$, 16 in $E_{\pm}$ and $\bar{E}_{\pm}$, and four in G_{+}, which altogether give the 81 independent angular distributions. This is of course just the number of components of the density matrix $\mathscr{P}^{\lambda\bar{\lambda}}_{\lambda'\bar{\lambda}'}$.

In principle one can imagine measuring all possible combinations of products of the nine helicity amplitudes, summed over initial polarizations. In practice, this

requires charge (flavor) identification of both the W^- and W^+ decay products. Although this is easy when both W's decay leptonically, these rates are rather small and one has the twofold identification ambiguity discussed in appendix B. Experimentally the most favorable mode is thus "semi-leptonic," with one W decaying leptonically, the other hadronically. In view of the difficulty of flavor identification, for most of the hadronic decays one cannot tell θ from $\pi - \theta$ ($\bar{\theta}$ from $\pi - \bar{\theta}$) and ϕ from $\phi + \pi$ ($\bar{\phi}$ from $\bar{\phi} + \pi$). This makes it very difficult to measure any of the coefficients in $D_\pm$ and one combination of the coefficients in A. Apart from these, there is a reasonable chance that one can determine the remaining 64 coefficients. We remark that the nontrivial azimuthal-angle correlation recently studied by Duncan, Kane, and Repko [29] is just one of these coefficients, $\mathrm{Re}\, G_-$.

In sect. 5, we will describe in some detail how to project out some of these coefficients experimentally, as a function of the scattering angle Θ. There we shall also discuss the accuracy with which they may be determined.

4.3. SYMMETRY PROPERTIES AND INCLUSIVE DISTRIBUTIONS

Although each of the 81 coefficients gives independent information on the W pair production mechanism, some of these coefficients may be related even in the presence of anomalous couplings. This is the case, for instance, if CP is a good symmetry or if no strong interactions exist in the W-boson sector. Even in models where one expects a strongly interacting W sector at high energies, one generally gets small WW interactions near the threshold, that is, at LEP-II energies. In contrast, C or P invariance do not lead to a useful classification, because the neutrino-exchange contribution to the amplitude violates C and P maximally, thereby hiding C and P invariance of the vector-boson sector.

Let us first examine the consequences of CP invariance. Since the relevant initial e^+e^- state is CP-invariant, the CP transformation simply reverses all the momenta of final particles and changes particles to antiparticles. Thus CP invariance leads to the following relation in the differential cross section

$$d\sigma(\Theta; \theta, \phi; \bar{\theta}, \bar{\phi}) \overset{CP}{=} d\sigma(\Theta; \pi - \bar{\theta}, \bar{\phi} + \pi; \pi - \theta, \phi + \pi). \tag{4.18}$$

In other words, the angular distributions which change sign under the exchange

$$(\theta, \phi, \bar{\theta}, \bar{\phi}) \overset{CP}{\leftrightarrow} (\pi - \bar{\theta}, \bar{\phi} + \pi, \pi - \theta, \phi + \pi) \tag{4.19}$$

are called CP-odd and should have vanishing coefficients if CP is a good symmetry. The terms which remain unchanged are called CP-even and can be nonzero. It is

straightforward to organize the 81 coefficients into 45 CP-even combinations and 36 CP-odd ones*.

Secondly, we study the implications of having only weak interactions among W's. The concomitant smallness of rescattering for the produced W pairs leads to small absorptive amplitudes. As is discussed in subsect. 3.4, if an amplitude has no absorptive part, CPT invariance gives the relation (3.9). We will refer to this symbolically as $CP\tilde{T}$ symmetry**. Thus the observation of a $CP\tilde{T}$-odd asymmetry would indicate the existence of rescattering effects. As a consequence of $CP\tilde{T}$ invariance we find

$$d\sigma(\Theta;\theta,\phi;\bar{\theta},\bar{\phi}) \overset{CP\tilde{T}}{=} d\sigma(\Theta;\pi-\bar{\theta},\pi-\bar{\phi};\pi-\theta,\pi-\phi). \tag{4.20}$$

We can easily separate the angular distributions into $CP\tilde{T}$-even and $CP\tilde{T}$-odd parts according to their behavior under the exchange

$$(\theta,\phi,\bar{\theta},\bar{\phi}) \overset{CP\tilde{T}}{\leftrightarrow} (\pi-\bar{\theta},\pi-\bar{\phi},\pi-\theta,\pi-\phi). \tag{4.21}$$

The eighty-one angular coefficients can thus be divided into four categories under CP and $CP\tilde{T}$: even-even, even-odd, odd-even, and odd-odd terms. CP-odd coefficients directly measure CP violation and $CP\tilde{T}$-odd terms indicate rescattering effects. Once both CP-odd and $CP\tilde{T}$-odd terms are found to be small experimentally, it is then safe to ignore odd-odd terms since they should be doubly suppressed.

With regard to these properties, we shall present a detailed study of three kinds of distributions which are more inclusive than the completely differential cross section (4.13). These are the azimuthal angle distributions after polar angle (θ and $\bar{\theta}$) integration, the polar angle correlations alter azimuthal angle integration, and the inclusive W^- and W^+ decay angular distributions (4.14).

After the integration over polar angles θ and $\bar{\theta}$, we can regard the 25 coefficients appearing in eq. (4.16) as functions of the scattering angle Θ only. Besides the trivial constant piece A, the remaining 24 azimuthal angle distributions are classified in table 5 according to their CP and $CP\tilde{T}$ properties. We find that all the *sine* terms are either CP-odd or $CP\tilde{T}$-odd whereas certain combinations of *cosine* terms are both CP- and $CP\tilde{T}$-odd. The standard model contributes exclusively to the even-even sector in the lowest (α^2) order. CP-even, $CP\tilde{T}$-odd terms*** are down by an

* In terms of helicity amplitudes, CP invariance reduces the number of independent amplitudes from nine to six (see eq. (3.13) and the footnote following thereafter), leading to $6 \times 6 = 36$ distributions. The remaining nine CP-even terms arise from a product of two CP-odd amplitudes, and may be ignored. Similar remarks also apply to the $CP\tilde{T}$ properties discussed below.

** When the interaction respects T invariance, we can similarly define observables which are proportional to rescattering effects. They are traditionally called T-odd quantities (see, e.g., ref. [51]). Here we use the term $CP\tilde{T}$ to avoid confusion with real CPT violation effects.

*** The one-loop Higgs contribution to these terms is calculated in ref. [52].

TABLE 5
CP and $CP\tilde{T}$ properties of azimuthal-angle distributions and correlations

CP	$CP\tilde{T}$	Azimuthal-angle distributions	Number
even	even	$\cos\phi - \cos\bar{\phi}, \cos 2\phi + \cos 2\bar{\phi}, \cos(\phi \pm \bar{\phi}),$ $\cos(\phi \pm 2\bar{\phi}) - \cos(\bar{\phi} \pm 2\phi), \cos(2\phi \pm 2\bar{\phi})$	8
even	odd	$\sin\phi - \sin\bar{\phi}, \sin 2\phi + \sin 2\bar{\phi}, \sin(\phi + \bar{\phi}),$ $\sin(\phi \pm 2\bar{\phi}) - \sin(\bar{\phi} \pm 2\phi), \sin(2\phi + 2\bar{\phi})$	6
odd	even	$\sin\phi + \sin\bar{\phi}, \sin 2\phi - \sin 2\bar{\phi}, \sin(\phi - \bar{\phi}),$ $\sin(\phi \pm 2\bar{\phi}) + \sin(\bar{\phi} \pm 2\phi), \sin(2\phi - 2\bar{\phi})$	6
odd	odd	$\cos\phi + \cos\bar{\phi}, \cos 2\phi - \cos 2\bar{\phi},$ $\cos(\phi \pm 2\bar{\phi}) + \cos(\bar{\phi} \pm 2\phi)$	4

additional factor of α, and *CP*-odd coefficients are even further suppressed. This structure is not changed by the introduction of *CP*-conserving anomalous couplings such as κ and λ.

If, on the other hand, one integrates over the azimuthal angles first, only the term A in eq. (4.16) remains. The surviving double polar angle distribution is given by eq. (4.17a). We can define the cross section for producing polarized W's by the coefficients $\mathscr{P}^{\lambda\bar{\lambda}}_{\lambda\bar{\lambda}}$ since they are nothing but the squared polarization amplitudes (see eq. (4.11)):

$$\frac{d\sigma(\lambda,\bar{\lambda})}{d\cos\Theta} = \frac{\beta}{128\pi s}\mathscr{P}^{\lambda\bar{\lambda}}_{\lambda\bar{\lambda}} \qquad (\lambda, \bar{\lambda} \text{ not summed}). \tag{4.22}$$

The nine cross sections can be easily projected out from the polar angle distribution (4.17a) which can be expressed as follows:

$$\frac{d\sigma}{d\cos\Theta\, d\cos\theta\, d\cos\bar{\theta}} = \frac{d\sigma(\lambda,\bar{\lambda})}{d\cos\Theta} B(W^- \to f_1\bar{f}_2) B(W^+ \to f_3\bar{f}_4) \tfrac{9}{16} d^2_{-\lambda} d^2_{-\bar{\lambda}}, \tag{4.23}$$

where now the summation over λ and $\bar{\lambda}$ should be performed. Among these nine cross sections, six combinations satisfy both *CP* and $CP\tilde{T}$, the remaining three violate both. They are listed in table 6.

TABLE 6
CP and $CP\tilde{T}$ properties of polar angle distributions

CP	$CP\tilde{T}$	Polarized W cross sections	Number
even	even	$\sigma(+,-), \sigma(-,+), \sigma(0,0),$ $\sigma(+,0) + \sigma(0,-), \sigma(-,0) + \sigma(0,+),$ $\sigma(+,+) + \sigma(-,-)$	6
odd	odd	$\sigma(+,0) - \sigma(0,-), \sigma(-,0) \cdots \sigma(0,+),$ $\sigma(+,+) - \sigma(-,-)$	3

Identification of all nine polarized W cross sections is difficult because of the necessity of double charge (flavor) identification. It is, however, possible to distinguish longitudinal W's from transverse ones without charge identification. Hence it is useful to define slightly more inclusive distributions

$$\frac{d\sigma_{TT}}{d\cos\Theta} = \sum_{\lambda=\pm}\sum_{\bar\lambda=\pm}\frac{d\sigma(\lambda,\bar\lambda)}{d\cos\Theta},$$

$$\frac{d\sigma_{LL}}{d\cos\Theta} = \frac{d\sigma(0,0)}{d\cos\Theta},$$

$$\frac{d\sigma_{TL}}{d\cos\Theta} = \sum_{\lambda=\pm}\frac{d\sigma(\lambda,0)}{d\cos\Theta},$$

$$\frac{d\sigma_{LT}}{d\cos\Theta} = \sum_{\bar\lambda=\pm}\frac{d\sigma(0,\bar\lambda)}{d\cos\Theta}, \tag{4.24}$$

and

$$\frac{d\sigma_T}{d\cos\Theta} = \frac{d\sigma_{TT}}{d\cos\Theta} + \frac{d\sigma_{TL}}{d\cos\Theta},$$

$$\frac{d\sigma_L}{d\cos\Theta} = \frac{d\sigma_{LT}}{d\cos\Theta} + \frac{d\sigma_{LL}}{d\cos\Theta},$$

$$\frac{d\sigma_{\bar T}}{d\cos\Theta} = \frac{d\sigma_{TT}}{d\cos\Theta} + \frac{d\sigma_{LT}}{d\cos\Theta},$$

$$\frac{d\sigma_{\bar L}}{d\cos\Theta} = \frac{d\sigma_{TL}}{d\cos\Theta} + \frac{d\sigma_{LL}}{d\cos\Theta}. \tag{4.25}$$

Some properties of these distributions have been studied in ref. [1].

Finally, the inclusive W^- or W^+ distributions (4.14) should be most useful when we study leptonic decay channels. We can parametrize these distributions as follows:

$$\frac{d\sigma(W^-\to\ell\bar\nu)}{d\cos\Theta\, d\cos\theta\, d\phi} = \sum_{i=1}^{9} F_i(\cos\Theta)L_i(\theta,\phi), \tag{4.26a}$$

$$\frac{d\sigma(W^+\to\bar\ell\nu)}{d\cos\Theta\, d\cos\bar\theta\, d\bar\phi} = \sum_{i=1}^{9} \bar F_i(\cos\Theta)L_i(\bar\theta,\bar\phi). \tag{4.26b}$$

Here the L_i's are the following nine orthogonal functions which are normalized to 4π:

$$L_1 = 1,$$

$$L_2 = \tfrac{1}{2}\sqrt{5}\,(1 - 3\cos^2\theta),$$

$$L_3 = \sqrt{3}\cos\theta,$$

$$L_4 = \sqrt{3}\sin\theta\cos\phi,$$

$$L_5 = \tfrac{1}{2}\sqrt{15}\sin 2\theta\cos\phi,$$

$$L_6 = \tfrac{1}{2}\sqrt{15}\sin^2\theta\cos 2\phi,$$

$$L_7 = \sqrt{3}\sin\theta\sin\phi,$$

$$L_8 = \tfrac{1}{2}\sqrt{15}\sin 2\theta\sin\phi,$$

$$L_9 = \tfrac{1}{2}\sqrt{15}\sin^2\theta\sin 2\phi. \tag{4.27}$$

Note that we have used the W^- scattering angle Θ in both F_i and $\bar{F}_i$. The coefficients F_1 and $\bar{F}_1$ are then proportional to the total inclusive angular distribution (4.15):

$$F_1(\cos\Theta) = \bar{F}_1(\cos\Theta) = \frac{B(W \to \ell\nu)}{4\pi}\frac{d\sigma}{d\cos\Theta}, \tag{4.28}$$

It is an elementary exercise to express the F_i's and $\bar{F}_i$'s in terms of our production tensors $\mathcal{P}^{\lambda\bar{\lambda}}_{\lambda'\bar{\lambda}'}$ and $\mathcal{P}^{\lambda\bar{\lambda}}_{\lambda\bar{\lambda}'}$, respectively. The CP and $CP\tilde{T}$ properties of these 18 coefficients are listed in table 7.

TABLE 7
CP and $CP\tilde{T}$ properties of inclusive W^- or W^+ decay angular distributions

CP	$CP\tilde{T}$	Inclusive angular coefficients	Number
even	even	$F_1 + \bar{F}_1, F_2 + \bar{F}_2, F_3 - \bar{F}_3$	6
		$F_4 - \bar{F}_4, F_5 + \bar{F}_5, F_6 + \bar{F}_6$	
even	odd	$F_7 - \bar{F}_7, F_8 + \bar{F}_8, F_9 + \bar{F}_9$	3
odd	even	$F_7 + \bar{F}_7, F_8 - \bar{F}_8, F_9 - \bar{F}_9$	3
odd	odd	$F_1 - \bar{F}_1, F_2 - \bar{F}_2, F_3 - \bar{F}_3$	6
		$F_4 + \bar{F}_4, F_5 - \bar{F}_5, F_6 - \bar{F}_6$	

See text for the definition of the coefficients F_i and $\bar{F}_i$. Note that $F_1 - \bar{F}_1$ is identically zero as long as CP violation in the decay process is neglected.

5. Observable consequences of anomalous three-vector-boson vertices

From the discussion of sect. 3, and in particular from table 4, it is apparent that different anomalous three-vector-boson vertices lead to deviations of different helicity amplitudes from their standard model values. In order to discover and then distinguish the anomalous couplings from each other, one thus has to separate the various helicity amplitudes. As has been discussed in the last section, the unique way of doing this is by studying angular distributions of the W^+ and W^- decay products.

Let us estimate the various experimental branching fractions. Consider the decay of each of the W's into a fermion-antifermion pair (quark-antiquark $q_1\bar{q}_2$ or charged lepton-neutrino $\ell^\pm\nu_\ell$) at tree level. Assuming a top quark of 40 GeV, the branching ratio for $W \to \ell\nu_\ell$ (ℓ= e, μ, or τ) is about 9% each. We thus expect the following final state combinations:

$$\begin{aligned} (q\bar{q})(q\bar{q}) &\Rightarrow \text{4-jet} && 53\%, \\ q\bar{q}(\ell\nu) &\Rightarrow \text{dijet} + \ell^\pm + \not{p} && 40\%, \\ (\ell\bar{\nu})(\bar{\ell}\nu) &\Rightarrow \ell^+\ell^- + \not{p} && 7\%, \end{aligned} \tag{5.1}$$

where $\not{p}$ stands for the momentum of the escaping neutrino(s). In this paper we shall mainly concentrate on the lepton + dijet decay mode*, because it is most amenable to a complete determination of angular distributions. However, to the extent that flavor and/or charge identification of the dijet subsystem is possible, the four-jet events can also contribute to the analysis. A very large fraction of all the W pair events can thus be used. Assuming a luminosity of LEP-II of 500 pb^{-1}/year and using $\sigma(e^+e^- \to W^+W^-) \sim 20$ pb at $\sqrt{s}$ = 190–200 GeV, one should have several thousand clean events per year, which is a statistically significant sample.

In the last section we gave a complete expression for the angular distribution of the two fermion-antifermion pairs arising from the decay of the W^+W^- pair. These angular distributions are particularly simple when measured in the rest frame of the parent W. Experimentally it is thus necessary to first identify the direction of the W axis which gives Θ, the angle of the W^- with respect to the e^- beam. The momenta of the decay products (the two jets and the charged lepton, say) then have to be boosted to their parent rest frames, which are moving with known velocities $\beta(W^\pm) = \mp(1 - 4m_W^2/s)^{1/2}$ along the axis. From the measurement of the opening angle between the two jets and the energy of both the charged lepton and the dijet

* In the clean environment of e^+e^- annihilation, the $\tau\nu$ decay of the W can be used as well as e/μ decays. The decay products of the τ are easy to identify. Because the τ mass is much smaller than the W mass, the direction of the final e/μ or hadrons from τ decay well approximates that of the parent τ. Although the energy of the τ cannot be measured directly, it can be calculated from other observable quantities using the kinematic constraints of the reaction.

system, it should be possible even to correct for initial radiation and finite width of both the W's.

Schematically, the differential cross section has the form (see eq. (4.13))

$$d\sigma \sim \sum_{i=1}^{81} \mathscr{P}_i(\Theta; s)\mathscr{D}_i(\theta, \phi, \bar{\theta}, \bar{\phi}). \tag{5.2}$$

Here the functions $\mathscr{D}_i$ form a linearly independent set consisting of low-order spherical harmonics, which reflects the known decay dynamics. The dynamics of the production process is solely contained in the factors $\mathscr{P}_i$. These are given essentially by the density matrix for the W pair, obtained from the helicity amplitudes. The fact that one can in principle measure 81 functions (instead of one for $d\sigma/d\cos\Theta$) shows that it is possible to extract an enormous amount of information on the production mechanism. Even though no polarization measurement is involved here, the parity-violating W decay provides a complete spin analyzer for the W.

With a few thousand events it is impossible to perform an 81-parameter fit (corresponding to the 81 angular coefficients in eqs. (4.16) and (4.17)) for each of several $\cos\Theta$ bins. Rather one would like to obtain from the experimental data the moments of those angular distributions that are most sensitive to new physics, i.e. the anomalous three-boson vertices for the case at hand.

The most sensitive distribution for any anomalous coupling will in general be some linear combination of the 81 angular distributions, whose coefficients depend on the W scattering angle Θ. It is in principle straightforward to maximize sensitivity for each coupling with respect to these 81 coefficients. Rather than pursuing such maximization, which would require detailed information on both detectors and actual event topologies, we have performed a systematic scan of all polar angle as well as azimuthal angle correlations and of all one-W-inclusive distributions.

In the following we mainly concentrate on the distributions which do not require double charge identification, because the charge of the parent quark of jets is difficult to measure. As seen from the discussion following (5.1), at least 40% of the events can be used to extract these distributions.

5.1. *CP*-CONSERVING COUPLINGS

A convenient way of organizing our findings is according to the sensitivity of the angular coefficients to *CP* violation and rescattering effects. We first discuss distributions which are even under the transformations (3.9) and (3.13) and thus in general are nonvanishing in the standard model at tree level. The couplings f_1, f_2, f_3, and f_5 are the ones to consider. Setting $g_1 = 1$ in $f_1 = g_1 + 2\gamma^2\lambda$ (eq. (2.5)), we shall take the more conventional quantities κ and λ, and f_5 as variables.

The simplest distribution of this kind is the differential cross section $d\sigma/d\cos\Theta$ which is given in fig. 7 for the standard model and for an anomalous "magnetic"

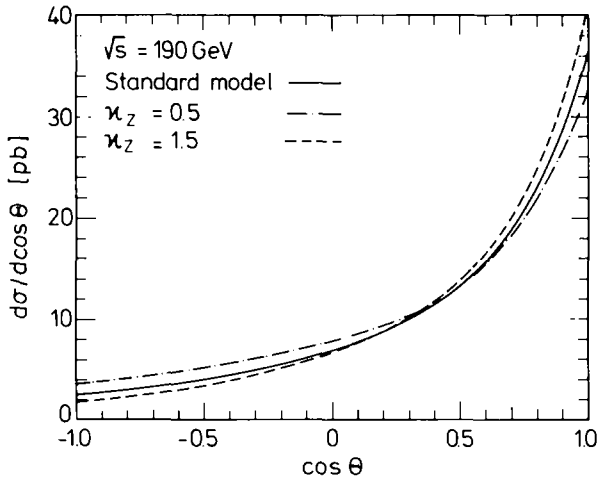

Fig. 7. Angular distribution $d\sigma/d\cos\Theta$ at $\sqrt{s} = 190$ GeV. Curves are shown for the standard model (solid line) and anomalous magnetic moments $\kappa_Z = 0.5$ (dash-dotted line) and $\kappa_Z = 1.5$ (dashed line). All the other couplings are as in the standard model.

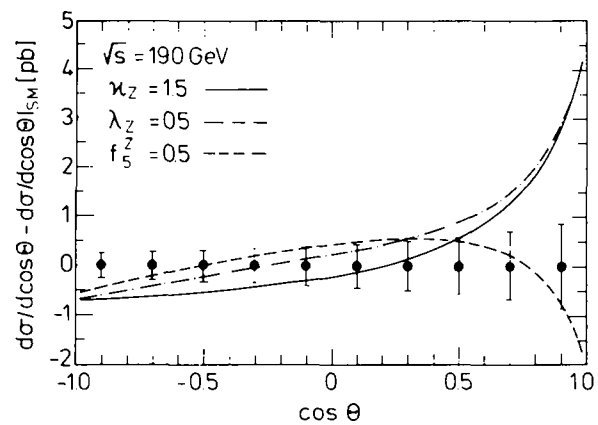

Fig. 8. Deviation of $d\sigma/d\cos\Theta$ from the standard model (SM) value for $\kappa_Z = 1.5$ (solid line), $\lambda_Z = 0.5$ (dash-dotted line), and $f_5^Z = 0.5$ (dashed line) at $\sqrt{s} = 190$ GeV. The error bars indicate the statistical error for 4000 W-pair events.

moment $\kappa_Z = 0.5$ and 1.5 at $\sqrt{s} = 190$ GeV*. The effect of the anomalous couplings is more clearly displayed in fig 8, where the deviation from the standard model is shown for $\kappa_Z = 1.5$, $\lambda_Z = 0.5$, and $f_5^Z = 0.5$ at the same energy. Comparing with the expected statistical error of the cross section measurement as shown by the error

* For all the numerical results in this paper we choose $m_W = 82$ GeV, $m_Z = 93$ GeV, $\sin^2\theta_w = 0.223$, and $e^2/4\pi = \alpha(m_W^2) = \frac{1}{128}$.

bars in fig. 8, we find that a deviation by 0.5 from the standard model value gives a very clean signal for κ_Z and λ_Z, while the effect is considerably smaller for f_5^Z.

The error bars in this and the following figures represent the statistical error for $N = 4000$ W-pair events in which one of the W's decays leptonically, and the other hadronically, thereby allowing single charge identification and a complete kinematical reconstruction. This number roughly corresponds to the production of 10^4 W-pair events (see the estimate (5.1)), expected with an integrated luminosity of 500 pb^{-1}. When a double charge identification for both W^- and W^+ decay products is required, only part of these 4000 events with clean heavy quark signals will be effective. On the other hand, a part of purely hadronic events can be useful with flavor identification and also purely leptonic decay channels can be used with the help of the kinematic reconstruction (appendix B). Since the statistical error scales as $1/\sqrt{N}$, it is easy to correct for these details as well as for detection inefficiencies.

By measuring the polar angle distribution of the W decay products, one can directly determine the differential cross section for fixed W helicities. From eq. (4.23) we obtain for example

$$\frac{d\sigma}{d\cos\Theta\, d\cos\theta} = \frac{d\sigma(\lambda = +)}{d\cos\Theta} \cdot \tfrac{3}{8}(1 - \cos\theta)^2 + \frac{d\sigma(\lambda = 0)}{d\cos\Theta} \cdot \tfrac{3}{4}\sin^2\theta + \frac{d\sigma(\lambda = -)}{d\cos\Theta} \cdot \tfrac{3}{8}(1 + \cos\theta)^2. \tag{5.3}$$

By projecting the experimental data onto $(1 \pm \cos\theta)^2$ and $\sin^2\theta$ for each $\cos\Theta$ bin (this can be achieved by taking the expectation values of $\frac{1}{2}(-1 \pm 2\cos\theta + 5\cos^2\theta)$ and $2 - 5\cos^2\theta$), one will thus obtain the differential cross section for fixed W^-

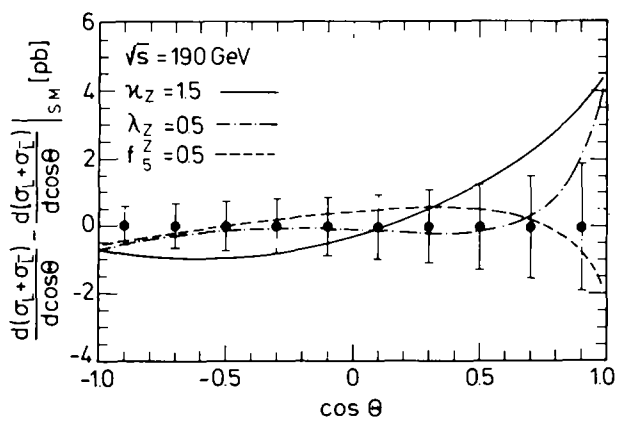

Fig. 9. Polar angle distribution for one of the W's being longitudinally polarized. Deviations from the standard model (SM) distribution are shown. Couplings and parametrization are chosen as in fig. 8. The error bars indicate the statistical error expected for 4000 W-pair events.

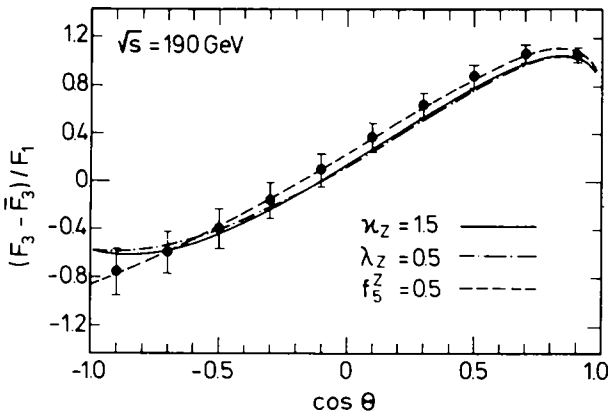

Fig. 10. W-scattering-angle dependence of $(F_3 - \bar{F}_3)/F_1$, the "sum" of forward-backward charge asymmetries (see eqs. (4.26) and (4.27)). Standard model predictions at $\sqrt{s} = 190$ GeV are shown by the solid circles with expected error bars based on 2000 $W^- \to \ell\bar{\nu}$ and 2000 $W^+ \to \bar{\ell}\nu$ events. The three curves denote predictions with $\kappa_Z = 1.5$ (solid line), $\lambda_Z = 0.5$ (dash-dotted line), and $f_5^Z = 0.5$ (dashed line).

helicities from the moments. Unfortunately, the cross sections (4.24) and (4.25) are in general not particularly sensitive to small deviations from the standard model couplings. The main exception we have found is $d(\sigma_L + \sigma_{\bar{L}})/d\cos\Theta$ (requiring either W^- or W^+ to be longitudinally polarized) which is reasonably sensitive to a variation of κ. Actually this quantity should make it possible to distinguish an anomaly in κ from others, as is demonstrated in fig. 9.

While the previous distributions only require distinction of W^+ from W^- decay products (to identify $\cos\Theta$), charge (or flavor) identification of the decay products gives their forward-backward asymmetry in the W rest frame. This asymmetry is, however, somewhat less sensitive to anomalous couplings than the previous distributions, as can be seen from fig. 10 where the sensitivity of the coefficient $(F_3 - \bar{F}_3)/F_1$ is shown. Incidentally, the strong charge asymmetry implies that the full polarization information on the W's is essential to reliably calculate the energy distribution of the charged leptons.

When the azimuthal angle of, say, the charged lepton is measured, new angular distributions can be obtained. Fig. 11 shows the sensitivity of $(F_4 - \bar{F}_4)/F_1$ to a variation of κ, λ, and f_5 (F_4 is the coefficient of $\sin\theta\cos\phi$, which is essentially the left-right asymmetry of the lepton; eq. (4.26)). It turns out that F_4 is only slightly less sensitive than $d\sigma/d\cos\Theta$ (fig. 7) to variations of order 0.5 of κ or λ from their standard model values. For smaller deviations from the standard model the relative sensitivity of these two distributions changes in favor of $d\sigma/d\cos\Theta$, due to the effect of terms quadratic in the anomalous couplings.

Additional flavor identification in the $\ell\nu$ plus dijet sample will increase the statistics for the inclusive W-decay distributions, because both W^+ and W^- decays can then be counted whereas the number of events contributing to $d\sigma/d\cos\Theta$

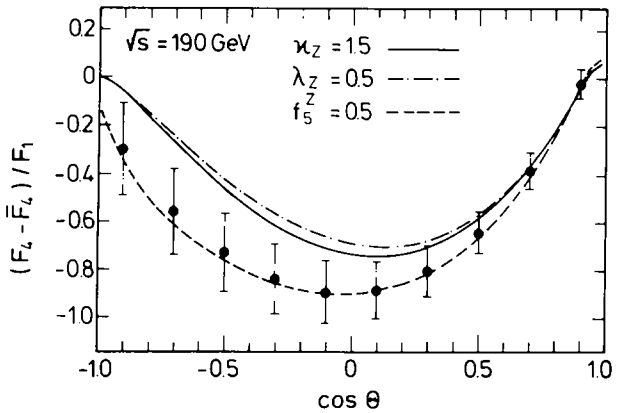

Fig. 11. W-scattering-angle dependence of $(F_4 - \bar{F}_4)/F_1$, the coefficient of $\sin\theta\cos\phi$ minus the coefficient of $\sin\bar{\theta}\cos\bar{\phi}$ (see eqs. (4.26) and (4.27)). Couplings and parameters are chosen as in fig. 10.

remains unchanged. For all the W^+ or W^- inclusive distributions, we show statistical errors on the basis of 2000 $W^- \to \ell\bar{\nu}$ and 2000 $W^+ \to \bar{\ell}\nu$ events only, neglecting any improvement from possible quark flavor identification.

It is clear from fig. 11 that the measurement of $F_4 - \bar{F}_4$ alone cannot distinguish between anomalies in κ and λ. This distinction is provided not only by the distribution $d(\sigma_L + \sigma_{\bar{L}})/d\cos\Theta$ (see fig. 9), but also by measuring in addition $(F_5 + \bar{F}_5)/F_1$ (F_5 is the coefficient of $\sin 2\theta\cos\phi$, or the quadrant asymmetry in the x-z plane; see eq. (4.26)), as demonstrated in fig. 12.

In all the distributions shown so far, sensitivity to the C- and P-violating coupling f_5 was much smaller than that for $\kappa - 1$ or λ. The reason for this is obvious when looking at table 4: in the amplitudes f_5 has a D-wave threshold and is suppressed

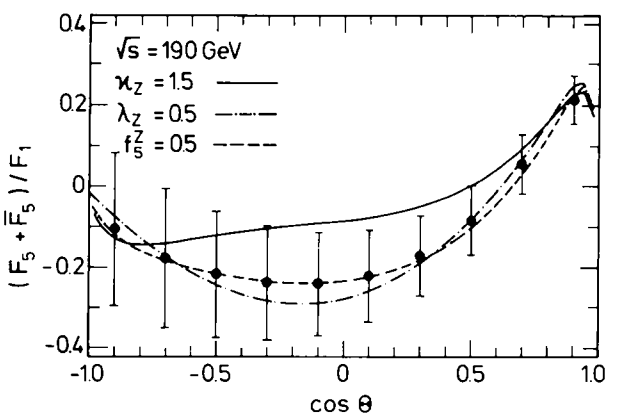

Fig. 12. W-scattering-angle dependence of $(F_5 + \bar{F}_5)/F_1$, the sum of the coefficient of $\sin 2\theta\cos\phi$ and that of $\sin 2\bar{\theta}\cos\bar{\phi}$ (see eqs. (4.26) and (4.27)). Couplings and parameters are the same as in fig. 10.

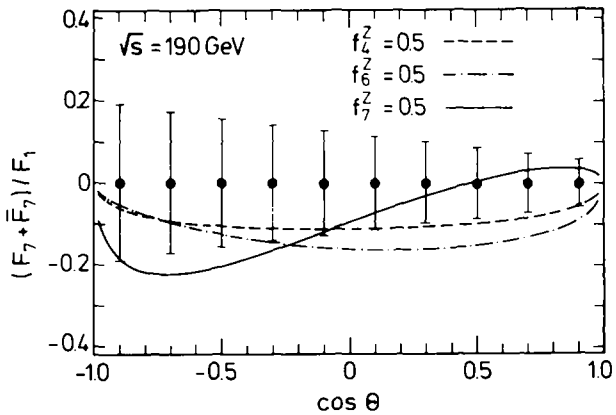

Fig. 13. W-scattering-angle dependence of $(F_7 + \bar{F}_7)/F_1$, the sum of the coefficient of $\sin\theta \sin\phi$ and that of $\sin\bar{\theta} \sin\bar{\phi}$ at $\sqrt{s} = 190$ GeV, for $f_4^Z = 0.5$ (dashed line), $f_6^Z = 0.5$ (dash-dotted line), and $f_7^Z = 0.5$ (solid line). The solid circles show the standard model expectation (zero), with the error bars indicating the expected statistical error for 2000 $W^- \to \ell^-\bar{\nu}$ and 2000 $W^- \to \ell^-\nu$ events.

by an extra factor $\beta \sim 0.5$ at $\sqrt{s} = 190$ GeV, $m_W = 82$ GeV. Better sensitivity to the coupling f_5 requires higher c.m. energies.

5.2. *CP*-VIOLATING COUPLINGS

As the next class of anomalous couplings we consider the *CP*-violating terms proportional to f_4, f_6, and f_7. Without absorptive parts, they contribute *imaginary* parts to the helicity amplitudes (see table 4). Provided that they are not so large, they have very little effect on "real" distributions*, such as $d\sigma/d\cos\Theta$, because in the standard-model amplitudes there is no large imaginary part to interfere with. A large sensitivity can only be obtained by measuring coefficients of *sines* of azimuthal angles, where the dynamical imaginary part from *CP* violation interferes with the relative phases between different helicity amplitudes.

The most sensitive measure appears to be the quantity $(F_7 + \bar{F}_7)/F_1$ (F_7 is the coefficient of $\sin\theta \sin\phi$; see eq. (4.26)), which is plotted for f_i^Z $(i = 4, 6, 7) = 0.5$ in fig. 13. It is essentially the up-down asymmetry of the lepton with respect to the scattering plane. A deviation from the standard model prediction (identically zero) is clearly visible for all these couplings with 4000 W-pair events with dijet + $\ell\nu$ topology.

While the dependence of the above quantity on the W scattering angle is distinct for f_7, separation of f_4 and f_6 may be achievable by studying some of the azimuthal correlations, namely, the coefficients of $\sin(\phi - 2\bar{\phi}) - \sin(2\phi - \bar{\phi})$ (fig. 14) or $\sin(\phi - \bar{\phi})$ (fig. 15) in the double decay distributions (see eq. (4.16)). However, the former

* When their absolute value becomes O(1), they do have measurable effects on e.g., $d\sigma/d\cos\Theta$, however.

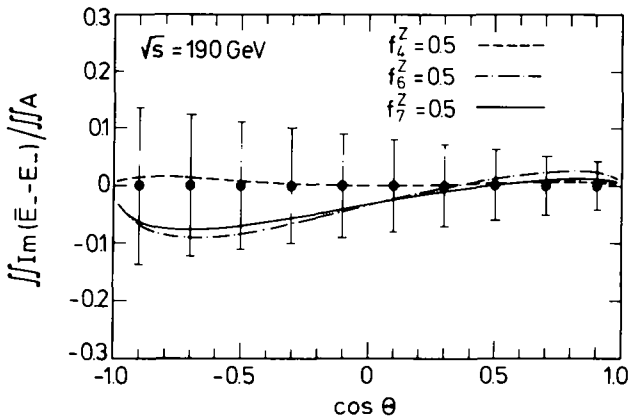

Fig. 14. W-scattering-angle dependence of the coefficient of $\sin(\phi - 2\bar{\phi}) + \sin(\bar{\phi} - 2\phi)$, i.e.

$$\int d\cos\theta \int d\cos\bar{\theta}\, \mathrm{Im}(\bar{E}_- - E_-) \Big/ \int d\cos\theta \int d\cos\bar{\theta}\, A$$

(see eqs. (4.16) and (4.17)) at $\sqrt{s} = 190$ GeV, for $f_4^Z = 0.5$ (dashed line), $f_6^Z = 0.5$ (dash-dotted line), and $f_7^Z = 0.5$ (solid line). The solid circles indicate the standard model value (zero), with statistical errors expected for 4000 W pairs where either W^- or W^+ decays leptonically.

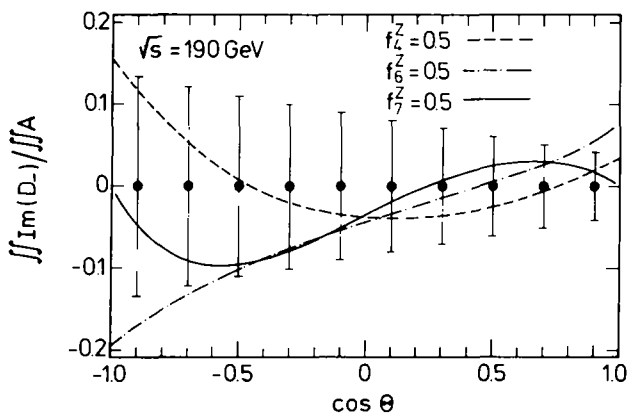

Fig. 15. Same as fig. 13 but for the coefficient of $\sin(\phi - \bar{\phi})$, i.e.

$$\int d\cos\theta \int d\cos\bar{\theta}\, \mathrm{Im}\, D_- \Big/ \int d\cos\theta \int d\cos\bar{\theta}\, A$$

(see eqs. (4.16) and (4.17)). Expected statistical errors are shown for 1000 W-pair events where the charges of both W-decay products are identified.

is not very sensitive to anomalous couplings, and the latter requires additional flavor identification, even when the charged lepton + dijet signal is considered. (This additional requirement has crudely been taken into account in the error bars of fig. 15, which are based on a sample of 1000 W pairs only.) Alternatively, a measurement near the WW threshold could single out f_6, because it is the only three-boson coupling that gives an S-wave threshold behavior.

It should be noted that the distributions shown in figs. 13–15 provide a genuine measure of *CP* violation in the vector-boson sector. Even with arbitrarily strong final-state interactions, all of them vanish as long as *CP* is conserved.

5.3. FINAL-STATE INTERACTIONS

In order to adequately treat rescattering effects, a partial wave analysis of the WW system is required. However, one can approximately include these effects by allowing for imaginary parts in the form factors f_i ($i = 1, \ldots, 7$). Tables 5–7 in sect. 4 give the distributions which are sensitive to rescattering, with and without *CP* violation. Here one example should suffice. Fig. 16 shows the effect of a small imaginary part of κ_Z ($\kappa_Z = 1 + 0.2i$) on $F_7 - \bar{F}_7$. (F_7 is the coefficient of $\sin\theta \sin\phi$ and $\bar{F}_7$ that of $\sin\bar{\theta} \sin\bar{\phi}$; see eq. (4.26).) It should be noticed that $F_7 - \bar{F}_7$ does vanish even in the presence of *CP* violation, as long as there are no absorptive parts.

A careful study of the angular distributions of W decay products thus provides a unique separation of anomalous effects into those due to strong final-state interactions, *CP* violation in the vector-boson couplings, or real anomalous moments of the W (such as κ or λ).

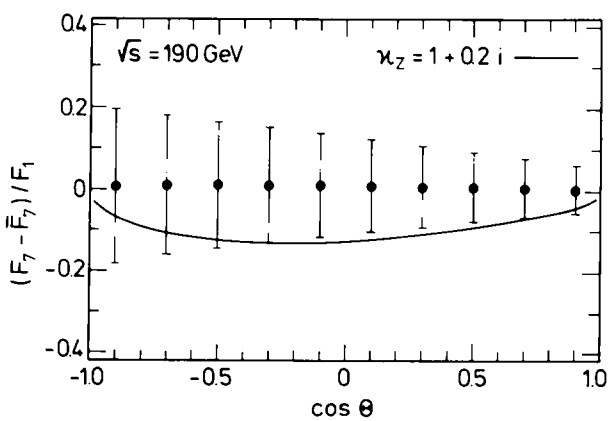

Fig. 16. Sensitivity of $F_7 - \bar{F}_7$ (the coefficient of $\sin\theta \sin\phi$ minus that of $\sin\bar{\theta} \sin\bar{\phi}$) to an imaginary part in κ_Z ($\kappa_Z = 1 + 0.2i$) at $\sqrt{s} = 190$ GeV. The solid circles show the standard model expectation, slightly away from zero due to the finite Z width (which is a part of one-loop electroweak corrections), with expected statistical errors for 2000 $W^- \to \ell\bar{\nu}$ and 2000 $W^+ \to \bar{\ell}\nu$ events.

5.4. PHOTON VERSUS Z COUPLINGS

So far we have only considered anomalous WWZ couplings. The question arises whether adding anomalous WWγ couplings as well may produce new features in angular distributions. The answer is *no* in the absence of *transverse* beam polarization. Let us explain this statement.

The differential cross section is a sum of contributions from left-handed ($\Delta\sigma = -1$) and right-handed ($+1$) electrons:

$$d\sigma \sim |\mathcal{M}_+|^2 + |\mathcal{M}_-|^2. \tag{5.4}$$

Adding photon and Z contributions, we deduce from eq. (3.7) that $\mathcal{M}_+$ and $\mathcal{M}_-$ are always proportional to the same linear combination of couplings f^γ and f^Z:

$$\mathcal{M}_+ \sim f^\gamma - \frac{s}{s - m_Z^2} f^Z$$

$$\equiv f^R = f^\gamma - 1.32 f^Z, \tag{5.5a}$$

$$\mathcal{M}_- \sim f^\gamma + \left(\frac{1}{2\sin^2\theta_w} - 1 \right) \frac{s}{s - m_Z^2} f^Z$$

$$\equiv f^L = f^\gamma + 1.63 f^Z, \tag{5.5b}$$

where the numerical value holds for $\sqrt{s} = 190$ GeV, $m_Z = 93$ GeV, and $\sin^2\theta_w = 0.223$. However, only the left-handed contribution (5.5b) can interfere with the neutrino-exchange graph which contributes the dominant part of the cross section. One thus finds a much larger sensitivity of almost all angular distributions to the combination f^L than to f^R. This effect is clearly demonstrated in fig. 17 for $\lambda_\gamma = 0.3$ and λ_Z adjusted such that either λ_R or λ_L vanishes. As a result it will be rather difficult to distinguish anomalous WWγ from WWZ couplings.

In principle, experiments with longitudinally polarized beams can measure f^R and f^L separately. However, since $|\mathcal{M}_+|^2$ is much smaller than $|\mathcal{M}_-|^2$ (the former is typically 10^{-2} of the latter at $\sqrt{s} = 190$ GeV after integration), the accuracy of the f^R measurements will be severely limited by statistics.

The best way out is provided by transverse beam polarization. When the $e^\pm$ beams have natural transverse polarizations $P_T^\pm$, the differential distribution eq. (5.4) changes to

$$d\sigma \sim |\mathcal{M}_+|^2 + |\mathcal{M}_-|^2 + P_T^+ P_T^- \{ 2\,\mathrm{Re}(\mathcal{M}_+^* \mathcal{M}_-)\cos 2\Phi + 2\,\mathrm{Im}(\mathcal{M}_+^* \mathcal{M}_-)\sin 2\Phi \}, \tag{5.6}$$

where Φ denotes the azimuthal angle of the W^- momentum about the e^- beam axis,

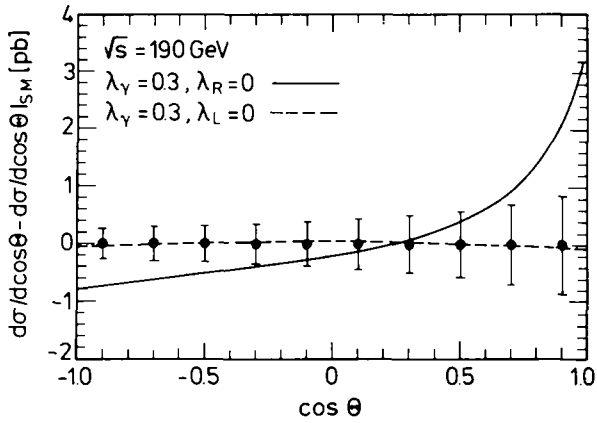

Fig. 17. Deviation of $d\sigma/d\cos\Theta$ from the standard model value at $\sqrt{s} = 190$ GeV. For $\lambda_\gamma = 0.3$, λ_Z is chosen such that either λ_R (the combination of λ_γ and λ_Z entering the amplitude for right-handed electrons, solid line) or λ_L (dashed line) vanishes. The error bars show statistical errors expected for 4000 W-pair events with either W^- or W^+ decaying leptonically.

measured from the e^- polarization direction in the e^+e^- c.m. frame*. The Φ-dependent terms contain the interference of the large neutrino-exchange amplitude with the right-handed amplitude (5.5a). One will thus obtain a much better measurement of f^R, which allows separation of f^γ from f^Z.

5.5. ENERGY DEPENDENCE

So far we have discussed various angular distributions only at a fixed beam energy $2E_b = \sqrt{s} = 190$ GeV. Actually their sensitivity to anomalous couplings strongly depends on $\sqrt{s}/m_W$, in particular near threshold. At low beam energies the photon and Z amplitudes are down by an extra factor of β compared to the neutrino exchange graph (see eq. (3.4)). Thus a small deviation of these amplitudes from their standard model values will be difficult to detect, with a notable exception of the *CP*-violating couplings f_6^V as mentioned earlier. When the beam energy and therefore $\gamma = E_b/m_W$ becomes large, the anomalous couplings will enhance the W pair amplitude because the subtle gauge-theory cancellation is switched off. However, γ^2 is only ≈ 1.5 even at $\sqrt{s} = 200$ GeV, the highest energy that LEP-II will be able to reach. Hence this enhancement effect will not be observable at LEP-II for the small ($O(\frac{1}{10})$) deviations from the standard model couplings that we are interested in.

* The distribution (5.6) can easily be obtained from the general expression in ref. [42] (see eq. (7.15) therein) by choosing the x-z plane to be the W pair production plane, as was done in sect. 3 to present explicit forms of the helicity amplitudes. It also can be directly read off from eq. (3.8) in ref. [53] with the replacement $P^2 \to P_T^+ P_T^-$. The difference in the sign comes from the different phase convention used.

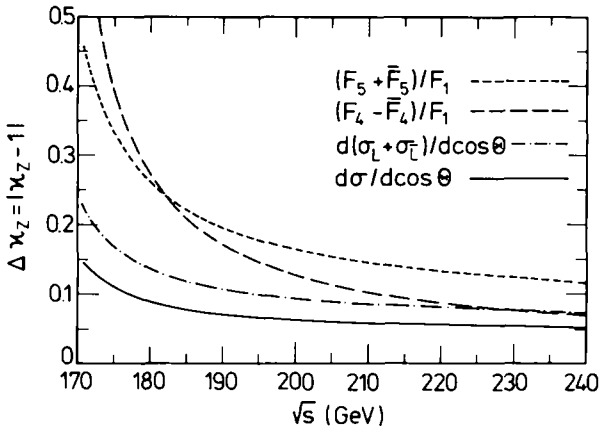

Fig. 18. Minimum deviation of κ_Z from its standard model value needed to produce a 1σ effect in the four most sensitive angular distributions as a function of the center-of-mass energy. The curves are for $d\sigma/d\cos\Theta$ (solid line), $(F_4 - \bar{F}_4)/F_1$ (dashed line), $d(\sigma_L + \sigma_{\bar{L}})/d\cos\Theta$ (dash-dotted line), and $(F_5 + \bar{F}_5)/F_1$ (short-dashed line).

We have made a rough estimate of the accuracy with which anomalous couplings can be determined as the c.m. energy varies. For an integrated luminosity of 500 pb^{-1} and assuming that 40% of all the W pairs can be used to determine angular distributions, we have plotted the deviations $\Delta\kappa_Z$ (fig. 18) and $\Delta\lambda_Z$ (fig. 19) needed to produce a 1σ effect in the most sensitive angular distributions. As is clearly seen from these figures, going beyond 200 GeV with $\sqrt{s}$ does not lead to a large increase of sensitivity. In the case of *CP*-conserving real anomalous couplings such as κ_Z and

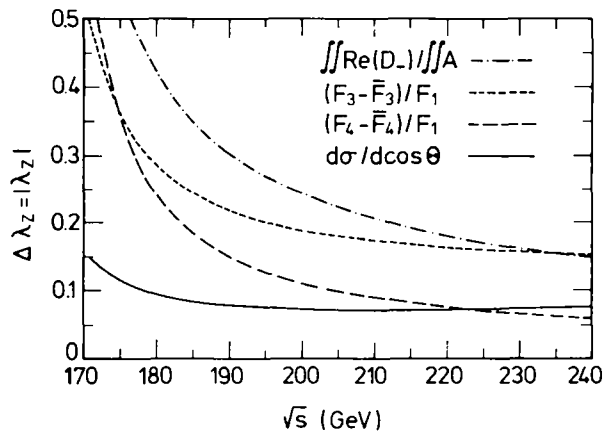

Fig. 19. Same as fig. 18 but for λ_Z. The curves give the sensitivities of $d\sigma/d\cos\Theta$ (solid line), $(F_4 - \bar{F}_4)/F_1$ (dashed line), the coefficient of $\cos(\phi - \bar{\phi})$ (dash-dotted line), and the forward-backward charge asymmetry of W decay products $(F_3 - \bar{F}_3)/F_1$ (short-dashed line).

λ_Z, the total angular distribution $d\sigma/d\cos\Theta$ (solid lines) is found to give the most sensitive measure. Other distributions are still useful to distinguish among effects from different anomalous couplings as discussed earlier in this section. If one uses only $d\sigma/d\cos\Theta$, we find almost no improvement beyond $\sqrt{s} = 190$ GeV. More generally, we find that a factor of 4 increase of luminosity at $\sqrt{s} = 190$ GeV is more valuable for measuring anomalous couplings than an increase of $\sqrt{s}$ to 200 GeV.

Figs. 18 and 19 show that λ or κ can be determined with an accuracy of ± 0.1 within one year of running at $\sqrt{s} = 190$ GeV. Thus a measurement of the "magnetic" moment of the W at the 5% level seems to be possible up to the γZ ambiguity addressed in subsect. 5.4. Similar results hold for the other couplings f_i ($i = 4, \ldots, 7$). After one year of running one is sensitive to variations Δf_i of roughly ± 0.1 except for f_5 which can be determined with an error of ± 0.2.

6. Conclusion

In this paper we have made a systematic study of observable experimental distributions connected with the process $e^+e^- \to W^+W^-$, which could serve as tests of possible anomalous three-vector-boson couplings. Since the W's decay into fermion-antifermion pairs, one may make use of the decay distributions as polarimeters to efficiently analyze the produced W helicities. Because the W decay properties are well known, a careful study of the reaction $e^+e^- \to W^+W^- \to f_1\bar{f}_2 f_3\bar{f}_4$ therefore reveals information on the W-pair production process and the associated three-vector-boson couplings, through the particular correlations produced for the final fermions.

More specifically, we have shown that at LEP-II it is feasible to search for anomalous moments $\kappa - 1$ or λ connected with the WWZ (or WWγ) vertex. For these couplings, whose presence does not violate any conservation laws, the most sensitive experimental measure turns out to be the differential angular distribution of the produced W's. For a sample of 10^4 W pairs at $\sqrt{s} = 190$ GeV at LEP-II one should be able to measure deviations in $\kappa - 1$ and λ at the 10% level. More specific angular correlations involving the final fermions are not as sensitive to those deviations. However, these distributions get affected differently by $\kappa - 1$ and λ (see, e.g., fig. 9) and supply information complementary to that provided by the W differential cross section.

The situation is radically different when one considers the effect of *CP*-violating anomalous three-boson couplings or imaginary parts of the form factors indicating strong WW rescattering effects. In these circumstances, even for sizable couplings, these effects are not particularly visible in the W angular distributions. However a careful study of the polar and azimuthal distributions of leptons and antileptons produced in W decays can be used to isolate these phenomena. If θ, ϕ and $\bar{\theta}, \bar{\phi}$ are the polar and azimuthal angles of the produced leptons and antileptons in W^- or W^+ decay, respectively, we have found that the terms proportional to $\sin\theta \sin\phi \pm$

$\sin\bar{\theta}\sin\bar{\phi}$ (lepton asymmetry with respect to the scattering plane) provide the most sensitive distributions for CP violation (+ sign) or rescattering effects (− sign).

Our detailed calculations considered the relevant processes $e^+e^- \to W^+W^-$, $W \to f\bar{f}$ only in the lowest order in the electroweak interactions. Obviously, a detailed study of possible anomalous contributions must include electroweak radiative corrections to be really significant. Because in our considerations we have treated the production process separate from the decay and mostly studied kinematical effects, it should be relatively straightforward to perform radiative corrections separately for the W^+W^- production and the decay. These corrections should modify our amplitudes in detail but not in overall structure. As an example, in appendix C, we have already indicated what modification arises if the hadronic W decay is not into $q\bar{q}$ but $q\bar{q}g$. At any rate, we believe that our calculations do indicate the approximate size of measurable effects at LEP-II.

We are grateful for many useful suggestions on these matters by the members of the LEP study group on high energies: G. Barbiellini, M. Davier, H.U. Martyn, B. Schrempp, F. Schrempp, and S. Yamada. K. Hagiwara wishes to thank J. Cortés for collaboration in the early stage of this work. K. Hikasa would like to thank Hidenaga Yamagishi for a stimulating collaboration carried out at the University of Tokyo, from which some of the results in this paper were obtained. He is also grateful to members of the DESY Theory Group for their hospitality. His work was supported in part by the University of Wisconsin Research Committee with funds granted by the Wisconsin Alumni Research Foundation, and in part by the US Department of Energy under contract DE-AC02-76ER00881.

Appendix A

CONSTRAINTS ON THE FORM FACTORS PARAMETRIZED BY GAEMERS AND GOUNARIS

The most general WWZ coupling for on-shell W's parametrized by Gaemers and Gounaris [12] (GG) contains nine form factors whereas we keep only seven in eq. (2.4). Explicitly, we find

$$\Gamma_V^{\alpha\beta\mu}|_{GG} = \Gamma_V^{\alpha\beta\mu}|_{(2.4)} + \frac{f_9^V - if_8^V}{m_W^2} P^\alpha [PQ]^{\mu\beta} + \frac{f_9^V + if_8^V}{m_W^2} P^\beta [PQ]^{\mu\alpha}, \quad \text{(A.1)}$$

where $Q^\nu = (q - \bar{q})^\nu$, and $[PQ]^{\mu\alpha}$ is a shorthand notation for $\varepsilon^{\mu\alpha\rho\sigma}P_\rho Q_\sigma$.

Spin counting and rotational invariance tell us that there are only seven independent helicity combinations, which are given explicitly in table 4. It is then clear that our seven form factors are enough to make all the helicity amplitudes arbitrary*. The nine form factors in eq. (A.1) should therefore be redundant.

* **Note added in proof**. The same observation was made by M. Gourdin, as communicated to us by K.J.F. Gaemers.

This can easily be seen as follows. Since no rank-5 completely antisymmetric tensor exists in four dimensions,

$$g_{\lambda\mu}\varepsilon_{\alpha\beta\rho\sigma} - g_{\lambda\alpha}\varepsilon_{\mu\beta\rho\sigma} + g_{\lambda\beta}\varepsilon_{\mu\alpha\rho\sigma} - g_{\lambda\rho}\varepsilon_{\mu\alpha\beta\sigma} + g_{\lambda\sigma}\varepsilon_{\mu\alpha\beta\rho} = 0. \tag{A.2}$$

By multiplying the above equation by $P^\lambda P^\rho Q^\sigma$ and $Q^\lambda P^\rho Q^\sigma$, we find

$$-P_\alpha[PQ]_{\mu\beta} + P_\beta[PQ]_{\mu\alpha} = s\varepsilon_{\mu\alpha\beta\rho}Q^\rho, \tag{A.3}$$

$$P_\alpha[PQ]_{\mu\beta} + P_\beta[PQ]_{\mu\alpha} = s\beta^2\varepsilon_{\mu\alpha\beta\rho}P^\rho - Q_\mu[PQ]_{\alpha\beta}. \tag{A.4}$$

Here we used $P^2 = s$, $P\cdot Q = 0$, and $Q^2 = -s\beta^2$. Terms proportional to P_μ, q_α, or $\bar{q}_\beta$ have been set to zero, because they correspond to the scalar component of the vector bosons and do not contribute to the process $e^+e^- \to W^+W^-$. Using the above equations in eq. (A.1) and recalling that

$$\Gamma_V^{\alpha\beta\mu}|_{(2.4)} = \cdots + if_5^V\varepsilon^{\mu\alpha\beta\rho}Q_\rho - f_6^V\varepsilon^{\mu\alpha\beta\rho}P_\rho - \frac{f_7^V}{m_W^2}Q^\mu[PQ]^{\alpha\beta}, \tag{A.5}$$

we immediately find

$$f_5^V = \left(f_5^V + 4\gamma^2 f_8^V\right)|_{GG}, \tag{A.6a}$$

$$f_6^V = \left(f_6^V - 4\gamma^2\beta^2 f_9^V\right)|_{GG}, \tag{A.6b}$$

$$f_7^V = \left(f_7^V + f_9^V\right)|_{GG}. \tag{A.6c}$$

With the above replacements, all the amplitudes presented in ref. [12] agree with ours.

Appendix B

KINEMATICS OF $e^+e^- \to W^+W^- \to (\ell\bar{\nu})(\bar{\ell}\nu)$

Purely leptonic decay modes of a W pair, although small in rate, give the cleanest signal of the W-pair production process in e^+e^- collisions:

$$\begin{aligned} e^-(k) + e^+(\bar{k}) \to\ & W^- \quad + \quad W^+ \\ & \hookrightarrow \ell(l) + \bar{\nu}(p_{\bar{\nu}}) \quad \hookrightarrow \bar{\ell}(\bar{l}) + \nu(p_\nu). \end{aligned} \tag{B.1}$$

This is observed experimentally as

$$e^- + e^+ \to \ell + \bar{\ell} + \text{missing energy-momentum}, \tag{B.2}$$

where the final lepton pair can be either one of $e\bar{e}$, $e\bar{\mu}$, $\mu\bar{e}$, or $\mu\bar{\mu}$. The four-momenta of the particles are given in parentheses. The observable dilepton distributions were studied rather extensively by Dicus and Kallianpur [28].

Because of the cleanliness of the signal, this process deserves close attention. A simple kinematical analysis, presented below, shows that the two unobserved neutrino momenta can be determined from the observed lepton momenta up to a twofold discrete ambiguity, in the limit where the W width and photon radiation are neglected. Under certain circumstances, e.g., when the contribution from one of the two kinematically possible configurations is negligible compared to the other, this makes it possible to perform the full angular correlation studies, as presented in sect. 5, even with this purely leptonic signal. Such an approach has been shown to be useful [39] in the $W\gamma$ production studies at hadron colliders, where the use of the W leptonic decay signal is inevitable to avoid large backgrounds and the neutrino longitudinal momentum can be determined up to a twofold discrete ambiguity.

The kinematics of the process (B.1) is determined by six angles, two for the scattering, and two each for the W decays. Since we observe the two three-momenta of the leptons, generically we have sufficient observables to fix the whole configuration. A twofold ambiguity occurs, however, because the solution involves a quadratic equation. Here we present an explicit solution for the two unobserved neutrino momenta $p_{\bar{\nu}}$ and p_ν in terms of the observed lepton momenta l and $\bar{l}$. We work in the e^+e^- c.m. frame and assume massless neutrinos.

It suffices to solve for the three-momentum $\boldsymbol{p}_{\bar{\nu}}$ because $p_{\bar{\nu}}^0 = |\boldsymbol{p}_{\bar{\nu}}|$ and p_ν is given by momentum conservation. As the W^- energy is equal to the beam energy E_b, we have

$$p_{\bar{\nu}}^0 = E_b - l_0, \tag{B.3}$$

or

$$\boldsymbol{p}_{\bar{\nu}}^2 = (E_b - l_0)^2. \tag{B.4}$$

A similar equation holds for the $W^+ \to \bar{\ell}\nu$ decay:

$$\boldsymbol{p}_\nu^2 = (E_b - \bar{l}_0)^2. \tag{B.5}$$

Using momentum conservation $\boldsymbol{p}_\nu = -(\boldsymbol{p}_{\bar{\nu}} + \boldsymbol{l} + \bar{\boldsymbol{l}})$ and eq. (B.4), this last equation can be rewritten in terms of $\boldsymbol{p}_{\bar{\nu}}$:

$$(\boldsymbol{l} + \bar{\boldsymbol{l}}) \cdot \boldsymbol{p}_{\bar{\nu}} = E_b(l_0 - \bar{l}_0) - l_0^2 - \boldsymbol{l} \cdot \bar{\boldsymbol{l}} + \tfrac{1}{2}(m_\ell^2 + m_{\bar{\ell}}^2). \tag{B.6}$$

The third constraint comes from the condition that the lepton-antineutrino system should have the mass of the W:

$$(l + p_{\bar{\nu}})^2 = m_W^2, \tag{B.7}$$

which gives

$$\mathbf{1}\cdot\boldsymbol{p}_{\bar{\nu}} = E_b l_0 - l_0^2 - \tfrac{1}{2}m_W^2 + \tfrac{1}{2}m_\ell^2 . \tag{B.8}$$

Eqs. (B.6) and (B.8) lead to

$$\bar{\mathbf{1}}\cdot\boldsymbol{p}_{\bar{\nu}} = -E_b l_0 - \mathbf{1}\cdot\bar{\mathbf{1}} + \tfrac{1}{2}m_W^2 + \tfrac{1}{2}m_\ell^2 . \tag{B.9}$$

The three conditions (B.4), (B.8), and (B.9) provide the solution for $\boldsymbol{p}_{\bar{\nu}}$. We rewrite the right-hand sides of these equations for the sake of clarity:

$$\boldsymbol{p}_{\bar{\nu}}^2 = L , \tag{B.4'}$$

$$\mathbf{1}\cdot\boldsymbol{p}_{\bar{\nu}} = M , \tag{B.8'}$$

$$\bar{\mathbf{1}}\cdot\boldsymbol{p}_{\bar{\nu}} = N . \tag{B.9'}$$

Let us assume, for the moment, that the two three-momenta $\mathbf{1}$ and $\bar{\mathbf{1}}$ are not parallel. Then we can expand $\boldsymbol{p}_{\bar{\nu}}$ in terms of the lepton momenta

$$\boldsymbol{p}_{\bar{\nu}} = a\mathbf{1} + b\bar{\mathbf{1}} + c\mathbf{1}\times\bar{\mathbf{1}} . \tag{B.10}$$

The two linear equations (B.8') and (B.9') constrain $\boldsymbol{p}_{\bar{\nu}}$ to lie on a line in three-dimensional space. They give

$$\begin{aligned} a\mathbf{1}^2 + b\mathbf{1}\cdot\bar{\mathbf{1}} &= M , \\ a\mathbf{1}\cdot\bar{\mathbf{1}} + b\bar{\mathbf{1}}^2 &= N , \end{aligned} \tag{B.11}$$

which can be explicitly solved:

$$\begin{pmatrix} a \\ b \end{pmatrix} = \frac{1}{\mathbf{1}^2\bar{\mathbf{1}}^2 - (\mathbf{1}\cdot\bar{\mathbf{1}})^2} \begin{pmatrix} \bar{\mathbf{1}}^2 & -\mathbf{1}\cdot\bar{\mathbf{1}} \\ -\mathbf{1}\cdot\bar{\mathbf{1}} & \mathbf{1}^2 \end{pmatrix} \begin{pmatrix} M \\ N \end{pmatrix} . \tag{B.12}$$

The remaining variable c is determined using (B.4'):

$$c^2 = \frac{1}{|\mathbf{1}\times\bar{\mathbf{1}}|^2}\left[L - a^2\mathbf{1}^2 - b^2\bar{\mathbf{1}}^2 - 2ab\mathbf{1}\cdot\bar{\mathbf{1}}\right] . \tag{B.13}$$

The sign of c cannot be determined. This explicitly exhibits the twofold discrete ambiguity we mentioned earlier. The inequality $c^2 > 0$ is expected to be violated only by finite W-width effects and by radiative corrections, and hence may serve as a test of the W-pair signal.

In the exceptional case where the two lepton momenta are parallel, one obtains a one-parameter family of solution for which the azimuthal angle of $\boldsymbol{p}_{\bar{\nu}}$ with respect to the lepton momentum is left undetermined.

Appendix C

HELICITY AMPLITUDES FOR EVENT SIMULATION

The angular correlation formulas presented in sect. 4 are quite useful for obtaining theoretical insight into the problem, and correctly take into account the correlations caused by W boson spins. However, they are still far from satisfactory if they are to be used as a basis for a realistic event generator*. In order to achieve the goal of precision tests of the standard model at LEP-II such as an accurate measurement of m_W, a test of electroweak radiative corrections in W pair production, and a direct measurement of the Cabibbo-Kobayashi-Maskawa matrix elements, it is essential to understand the event topology of each W decay mode as much as possible.

First of all, it is important to include final quark mass effects for the $W^- \to b\bar{t}$ mode. At least one hard gluon emission should also be incorporated exactly in addition to the leading logarithmic multigluon emission which can easily be simulated at the classical level by using a QCD shower Monte Carlo program [54]. Although it is possible to present a complete polarization-summed cross section with the above effects included in the usual density matrix technique, the results turn out to be quite cumbersome since we need the double density matrix for W^- and W^+ decays. We find it most convenient to present our results for helicity amplitudes in the formalism [42] recently developed by two of us, where the final expression allows efficient and straightforward numerical evaluation in an arbitrary Lorentz frame. In this approach, it becomes trivial to incorporate an arbitrary polarization of the colliding beams (in particular the natural transverse polarization in storage rings), and it is easy to add new contributions such as a t-channel exchange of an excited neutrino [55] or a contact eeWW interaction. It is also straightforward to include final state polarization effects, e.g. of top quarks [56].

In order to render this paper self-contained we first briefly review the basic ingredients of the helicity basis calculus. Further details can be found in ref. [42].

For fermions we use the chiral representation of Dirac matrices and go to two-component notation. Spinors $\psi(=u(p,\lambda)$ or $v(p,\lambda))$ are given by

$$\psi = \begin{pmatrix} \psi_- \\ \psi_+ \end{pmatrix}; \qquad \bar{\psi} = \begin{pmatrix} \psi_+^\dagger & \psi_-^\dagger \end{pmatrix}, \tag{C.1}$$

with

$$\begin{aligned} u(p,\lambda)_\pm &= \omega_{\pm\lambda}(p)\chi_\lambda(p), \\ v(p,\lambda)_\pm &= \pm\lambda\omega_{\mp\lambda}(p)\chi_{-\lambda}(p). \end{aligned} \tag{C.2}$$

Here λ denotes the helicity of the on-shell fermion with four-momentum $p^\mu =$

* An event generator based on the formulas of this appendix is available from one of the authors (D.Z.).

(E, p_x, p_y, p_z), $\chi_\lambda(p)$ is a normalized helicity eigenspinor, explicitly given by

$$\chi_+(p) = [2|\boldsymbol{p}|(|\boldsymbol{p}| + p_z)]^{-1/2}\begin{pmatrix} |\boldsymbol{p}| + p_z \\ p_x + ip_y \end{pmatrix}, \tag{C.3a}$$

$$\chi_-(p) = [2|\boldsymbol{p}|(|\boldsymbol{p}| + p_z)]^{-1/2}\begin{pmatrix} -p_x + ip_y \\ |\boldsymbol{p}| + p_z \end{pmatrix}, \tag{C.3b}$$

and

$$\omega_\pm(p) = [E \pm |\boldsymbol{p}|]^{1/2}. \tag{C.4}$$

Given the explicit form of γ-matrices

$$\not{a} = a_\mu\gamma^\mu = \begin{pmatrix} 0 & \not{a}_+ \\ \not{a}_- & 0 \end{pmatrix}, \tag{C.5}$$

with

$$\not{a}_\pm = \begin{pmatrix} a^0 \mp a^3 & \mp(a^1 - ia^2) \\ \mp(a^1 + ia^2) & a^0 \pm a^3 \end{pmatrix}, \tag{C.6}$$

an arbitrary product of γ-matrices with spinors at both ends can be expressed by the basic quantity

$$S(p_i, a_1, \ldots, a_n, p_j)^\alpha_{\lambda_i\lambda_j} = \chi^\dagger_{\lambda_i}(p_i)(\not{a}_1)_\alpha(\not{a}_2)_{-\alpha}(\not{a}_3)_\alpha \cdots (\not{a}_n)_{\varepsilon\alpha}\chi_{\lambda_j}(p_j) \tag{C.7}$$

for $\alpha = \pm$ [here $\varepsilon = (-1)^{n-1}$]. Arbitrary polarization amplitudes are then expressed in terms of the basic quantity S, which is easily evaluated by 2×2 matrix multiplication*.

Analogous to eq. (C.2) for spin-$\frac{1}{2}$ fermions, polarization vectors for vector bosons are defined such that they depend only on the vector boson four-momentum $q = (q_0, q_x, q_y, q_z)$. We define the rectangular polarization basis by

$$\varepsilon^\mu(q, \lambda = 1) = \frac{1}{|\boldsymbol{q}|q_T}\left(0, q_xq_z, q_yq_z, -q_T^2\right), \tag{C.8a}$$

$$\varepsilon^\mu(q, \lambda = 2) = \frac{1}{q_T}(0, -q_y, q_x, 0), \tag{C.8b}$$

$$\varepsilon^\mu(q, \lambda = 3) = \frac{q_0}{\sqrt{q^2}|\boldsymbol{q}|}\left(\frac{\boldsymbol{q}^2}{q_0}, q_x, q_y, q_z\right), \tag{C.8c}$$

$$\varepsilon^\mu(q, \lambda = 4) = \frac{1}{\sqrt{q^2}}(q_0, q_x, q_y, q_z), \tag{C.8d}$$

* A simple FORTRAN program to evaluate the complex number S as a function of an arbitrary number of four momenta and three indices $(\alpha, \lambda_i, \lambda_j)$ is available from the authors of ref. [42].

with $q_T = (q_x^2 + q_y^2)^{1/2}$. In the usual helicity basis, the polarization vector (C.8c) describes longitudinally polarized vector bosons with helicity $\lambda = 0$, and helicity eigenvectors for $\lambda = \pm$ are given by

$$\varepsilon^\mu(q, \lambda = \pm) = \sqrt{\tfrac{1}{2}}\,[\mp\varepsilon^\mu(q, \lambda = 1) - i\varepsilon^\mu(q, \lambda = 2)]\,. \tag{C.9}$$

The $\lambda = 4$ component, which is proportional to q^μ, corresponds to the scalar part of a *virtual* vector boson. Its coupling to fermions is proportional to fermion masses and hence will be important only in the $b\bar{t}$ decay of virtual W's. We find no advantage of using the helicity basis for intermediate W's in numerical simulation and will choose the cartesian basis (C.8). One can, of course, obtain identical final cross sections using the helicity basis ($\lambda = \pm, 0, 4$) in summations.

In terms of the fermion strings S and the polarization vectors (C.8) or (C.9), we can now give the polarization amplitudes for the production process

$$e^-(k, \sigma) + e^+(\bar{k}, \bar{\sigma}) \to W^-(q, \lambda) + W^+(\bar{q}, \bar{\lambda})\,, \tag{C.10}$$

which in contrast to eqs. (3.2)–(3.6) are Lorentz covariant. For the neutrino exchange graph depicted in fig. 1c we obtain

$$\mathcal{M}^\nu(\sigma, \bar{\sigma}; \lambda, \bar{\lambda}) = \frac{e^2\left(g_-^{We\nu}\right)^2}{(k-q)^2}\delta_{\sigma,-}\delta_{\bar{\sigma},+}2\sqrt{k^0\bar{k}^0}\,S(\bar{k}, \varepsilon^*(\bar{\lambda}), k-q, \varepsilon^*(\lambda), k)^{-}_{--}\,. \tag{C.11}$$

The analogous expression for s-channel vector exchange is

$$\mathcal{M}^{\mathrm{V}}(\sigma, \bar{\sigma}; \lambda, \bar{\lambda}) = \frac{e g_\sigma^{\mathrm{Vee}} g_{\mathrm{WWV}}}{s - m_{\mathrm{V}}^2}\delta_{\sigma,-\bar{\sigma}}2\sqrt{k^0\bar{k}^0}\,S(\bar{k}, \Gamma_{\mathrm{V}}(\lambda, \bar{\lambda}), k)^{\sigma}_{\sigma\sigma}\,, \tag{C.12}$$

for $\mathrm{V} = \gamma$ and Z. The four-vector Γ_{V}^μ is obtained from the tensor $\Gamma_{\mathrm{V}}^{\alpha\beta\mu}$ of eq. (2.4) by contraction with the W polarization vectors

$$\Gamma_{\mathrm{V}}^\mu(\lambda, \bar{\lambda}) = \Gamma_{\mathrm{V}}^{\alpha\beta\mu}(q, \bar{q}, P)\varepsilon_\alpha^*(q, \lambda)\varepsilon_\beta^*(\bar{q}, \bar{\lambda})\,. \tag{C.13}$$

The WWγ and WWZ couplings g_{WWV} are given in eq. (2.6). The left- and right-handed fermion couplings to vector bosons are defined by the interaction lagrangian

$$\mathcal{L}_{Vf_1f_2} = -e\sum_{\lambda=\pm} g_\lambda^{\mathrm{V}f_1f_2}\bar{\psi}_{f_1}\gamma_\mu P_\lambda\psi_{f_2}V^\mu\,, \tag{C.14}$$

where e denotes the positron charge and $P_\lambda = \frac{1}{2}(1 + \lambda\gamma_5)$ is the chiral projection.

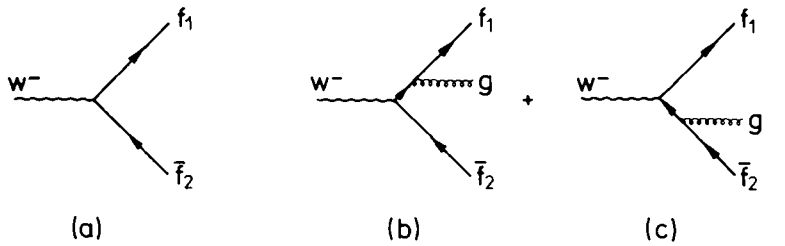

Fig. 20. Feynman diagrams for the decay processes (a) $W^- \to f_1\bar{f}_2$ and (b), (c) $W^- \to f_1\bar{f}_2 g$ at tree level.

The couplings we need are

$$
\begin{aligned}
g_{\pm}^{\gamma ee} &= -1, \\
g_{-}^{Zee} &= -\frac{1}{2\sin\theta_w\cos\theta_w} + \tan\theta_w, \\
g_{+}^{Zee} &= \tan\theta_w, \\
g_{-}^{We\nu} &= g_{-}^{We\nu} = \frac{1}{\sqrt{2}\sin\theta_w}, \\
g_{-}^{Wu_id_j} &= \left(g^{Wd_ju_i}\right)^* = \frac{U_{ij}}{\sqrt{2}\sin\theta_w},
\end{aligned}
\tag{C.15}
$$

where $(u_1, u_2, u_3) = (u, c, t)$, $(d_1, d_2, d_3) = (d, s, b)$, and U_{ij} denotes the Cabibbo-Kobayashi-Maskawa matrix elements for three generations.

Using the same notation as before, the decay matrix elements for $W^\pm \to f_1\bar{f}_2$ or $f_1\bar{f}_2 g$ depicted in fig. 20 can easily be written down. Denoting the fermion momenta and helicities by (p_1, σ_1) and (p_2, σ_2) one finds for the W^- decays

$$
\mathcal{M}^{(W^- \to f_1\bar{f}_2)}(\lambda; \sigma_1, \sigma_2) = e g_{-}^{Wf_1f_2} C \omega_{-\sigma_1}(p_1)\omega_{\sigma_2}(p_2)\sigma_2 S(p_1, \varepsilon(q,\lambda), p_2)^{-}_{\sigma_1, -\sigma_2},
\tag{C.16}
$$

and

$$
\begin{aligned}
&\mathcal{M}^{(W^- \to f_1\bar{f}_2 g)}(\lambda; \sigma_1, \sigma_2, \kappa) \\
&\quad = e g_{-}^{Wf_1f_2} g_s C' \omega_{-\sigma_1}(p_1)\omega_{\sigma_2}(p_2)\sigma_2 \\
&\qquad \times \left\{ \left[\frac{\varepsilon^*(p_g,\kappa)\cdot p_1}{p_g\cdot p_1} - \frac{\varepsilon^*(p_g,\kappa)\cdot p_2}{p_g\cdot p_2} \right] S(p_1, \varepsilon(q,\lambda), p_2)^{-}_{\sigma_1, -\sigma_2} \right. \\
&\qquad\quad + \frac{1}{2p_g\cdot p_1} S(p_1, \varepsilon^*(p_g,\kappa), p_g, \varepsilon(q,\lambda), p_2)^{-}_{\sigma_1, -\sigma_2} \\
&\qquad\quad \left. - \frac{1}{2p_g\cdot p_2} S(p_1, \varepsilon(q,\lambda), p_g, \varepsilon^*(p_g,\kappa), p_2)^{-}_{\sigma_1, -\sigma_2} \right\}.
\end{aligned}
\tag{C.17}
$$

Here we employ the gluon polarization vector $\varepsilon^\mu(p_g, \kappa)$ with $\kappa = 1$, 2 or $\pm$ for massless gluons. $g_s = \sqrt{4\pi\alpha_s}$ is the QCD coupling constant, and the effective color factors are

$$C = \begin{cases} \sqrt{N} = \sqrt{3} & \text{for quarks,} \\ 1 & \text{for leptons,} \end{cases} \tag{C.18a}$$

$$C' = \sqrt{C_F N} = 2 \qquad \text{for quarks.} \tag{C.18b}$$

These factors automatically take care of color summations in the final states. For W^+ decay one merely needs to substitute $\varepsilon(q, \lambda) \to \varepsilon(\bar{q}, \bar{\lambda})$ in both eqs. (C.16) and (C.17). Formulas (C.16) and (C.17) are valid for arbitrary masses of the fermions f_1 and $\bar{f}_2$. When fermion masses can be neglected, the ω-factors simplify to

$$\omega_{\pm\sigma}(p) \overset{p^2 \to 0}{\to} \sqrt{2p^0}\,\delta_{\sigma,\pm}. \tag{C.19}$$

We should note that the simple formulas (C.11) and (C.12) contain all the information regarding the process $e^+e^- \to W^+W^-$ in lowest order, and that the formulas (C.16) and (C.17) alone include the complete description of polarized W decay into a quark pair of arbitrary masses and an additional hard gluon. In sect. 3, we have shown explicit analytic expressions of the production amplitudes in the e^+e^- c.m. frame, whereas in sect. 4 we evaluated (C.16) in the W rest frame for massless fermions. The implicit expressions given in this appendix allow, however, a direct numerical evaluation of all the amplitudes in an arbitrary Lorentz frame. Since the individual amplitudes transform nontrivially under boosts, the Lorentz invariance of the polarization-summed squared amplitudes gives an excellent test of a numerical program [42].

The procedure to evaluate cross sections from these amplitudes is essentially the same as that explained in sect. 4. $\mathcal{M}_1$ is just the sum of $\mathcal{M}^\nu$ (C.11), $\mathcal{M}^\gamma$ and $\mathcal{M}^Z$ (C.12), $\mathcal{M}_2$ and $\mathcal{M}_3$ are either (C.16) or (C.17) depending on whether one wants to include the possibility of hard gluon emission. Only one further complexity appears when one deals with the decay mode $W \to b\bar{t}$. In this case the scalar ($\lambda = 4$) component of the W polarization cannot be neglected for off-mass-shell W's and the W polarization sum should be extended to

$$\sum_{\lambda=1,2,3} \to \sum_{\lambda=1,2,3} + \sum_{\lambda=4} \frac{q^2 - m_W^2}{m_W^2} \equiv \sum_{\lambda}^{U}, \tag{C.20}$$

which arises from the Proca (or unitary gauge) spin projector $-g_{\mu\nu} + q_\mu q_\nu / m_W^2$.

As an example, we give the exclusive cross section for the case

$$\begin{aligned} e^-(k,\sigma) + e^+(\bar{k},\bar{\sigma}) &\to W^-(q,\lambda) + W^+(\bar{q},\bar{\lambda}), \\ W^-(q,\lambda) &\to b(p_1,\sigma_1) + \bar{t}(p_2,\sigma_2) + g(p_3,\sigma_3), \\ W^+(\bar{q},\bar{\lambda}) &\to \bar{\ell}(p_4,\sigma_4) + \nu(p_5,\sigma_5). \end{aligned} \tag{C.21}$$

The full amplitude can be written

$$\begin{aligned} \mathcal{M} &= \mathcal{M}(\sigma,\bar{\sigma};\sigma_1,\sigma_2,\sigma_3;\sigma_4,\sigma_5) \\ &= D_W(q^2) D_W(\bar{q}^2) \sum_{\lambda}^{U} \sum_{\bar{\lambda}} \\ &\quad \times \mathcal{M}_1(\sigma,\bar{\sigma};\lambda,\bar{\lambda}) \mathcal{M}_2(\lambda;\sigma_1,\sigma_2,\sigma_3) \mathcal{M}_3(\bar{\lambda};\sigma_4,\sigma_5), \end{aligned} \tag{C.22}$$

where we show only particle polarization indices to denote each amplitude. For a given set of four-momenta of particles and their polarizations, all $\mathcal{M}_i$ and hence the total amplitude $\mathcal{M}$ is just a complex number.

The polarization-averaged cross section for the process (C.21) is then obtained simply by the following formula:

$$d\sigma = \frac{1}{2s} \cdot \tfrac{1}{4} \sum |\mathcal{M}|^2 \, d\Phi_5, \tag{C.23a}$$

with $d\Phi_5$ being the invariant five-body phase space

$$d\Phi_5 = (2\pi)^4 \delta^4\left(k + \bar{k} - \sum_{i=1}^{5} p_i\right) \prod_{i=1}^{5} \frac{d^3 p_i}{(2\pi)^3 2E_i}, \tag{C.23b}$$

and

$$\sum |\mathcal{M}|^2 = \sum_{\sigma=\pm} \sum_{\sigma_1=\pm} \sum_{\sigma_2=\pm} \sum_{\sigma_3=1}^{2} |\mathcal{M}|^2. \tag{C.23c}$$

Here we used the fact that $\mathcal{M}_1$ is proportional to $\delta_{\sigma,-\bar{\sigma}}$ (see (C.11) and (C.12)), and that $\mathcal{M}_3$ is proportional to $\delta_{\sigma_4,-}\delta_{\sigma_5,-}$ ((C.16) and (C.19)). If we can neglect the b quark mass, summation on the b spin is reduced to a single value $\sigma_1 = -$ for the standard V − A interactions. In the Monte Carlo event generation, one can perform not only the phase space integration but also the polarization sum on a statistical basis.

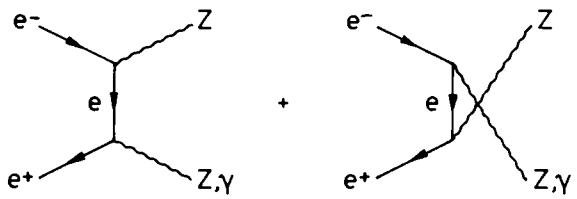

Fig. 21. Feynman diagrams for the processes $e^+e^- \to ZZ$ and $e^+e^- \to Z\gamma$ in the standard model.

Appendix D

HELICITY AMPLITUDES FOR $e^+e^- \to ZZ$ AND $e^+e^- \to Z\gamma$

Unlike W^+W^- production, ZZ and $Z\gamma$ production proceed only by well known fermion-vector-boson couplings in the leading order of the standard model (see fig. 21). Effects of the WWV coupling (2.1) appear only at the $O(\alpha)$ level [57,58]. Anomalous interactions of three neutral bosons [59], however, may contribute to the reactions. $Z\gamma$ production can be studied already at LEP-I/SLC at energies above the Z resonance, and ZZ production is within the reach of LEP-II. The latter reaction contributes [1] as a background to the Higgs boson search using the ZH final state when $m_H \sim m_Z$.

In this appendix we present helicity amplitudes for these processes

$$e^-(k,\sigma) + e^+(\bar{k},\bar{\sigma}) \to V_1(q_1,\lambda_1) + V_2(q_2,\lambda_2), \tag{D.1}$$

where V_1V_2 denote ZZ or $Z\gamma$. We include the most general ZZZ, ZZγ, and Z$\gamma\gamma$ couplings in the same spirit as that of our WWV coupling studies. We also give the $Z \to f\bar{f}$ and $Z \to f\bar{f}g$ decay amplitudes with arbitrary fermion masses. By combining these amplitudes, it is straightforward to make numerical simulations for processes such as $e^+e^- \to (Z \to \ell\bar{\ell}) + (Z \to t\bar{t}g)$, with full polarization correlations included.

In the standard model, only t- and u-channel electron exchange contribute to the processes. The corresponding production matrix element is

$$\begin{aligned}\mathcal{M}(\sigma,\bar{\sigma};\lambda_1,\lambda_2) = {} & e^2 g_\sigma^{V_1 ee} g_{\bar{\sigma}}^{V_2 ee} \delta_{\sigma,-\bar{\sigma}} 2\sqrt{k^0 \bar{k}^0} \\ & \times \left\{ \frac{S(\bar{k},\varepsilon^*(q_2,\lambda_2),k-q_1,\varepsilon^*(q_1,\lambda_1),k)^{\sigma}_{\sigma\sigma}}{(k-q_1)^2} \right. \\ & \left. + \frac{S(\bar{k},\varepsilon^*(q_1,\lambda_1),k-q_2,\varepsilon^*(q_2,\lambda_2),k)^{\sigma}_{\sigma\sigma}}{(k-q_2)^2} \right\}. \end{aligned} \tag{D.2}$$

As before (see eqs. (C.14) and (C.15)) $g_{\mp}^{V_i ee}$ denote the left- and right-handed couplings of electrons to the vector boson V_i.

The explicit form of the helicity amplitudes for $e^+e^- \to ZZ$ in the e^+e^- c.m. frame reads

$$\mathcal{M}^{(e^+e^- \to ZZ)} = 4\sqrt{2}\, e^2 \left(g_{\Delta\sigma}^{Zee}\right)^2 \delta_{|\Delta\sigma|,\,\pm 1} \frac{\mathscr{A}_{\lambda_1\lambda_2}(\Theta)}{4\beta^2 \sin^2\Theta + \gamma^{-4}} \varepsilon d^{J_0}_{\Delta\sigma,\Delta\lambda}(\Theta), \quad \text{(D.3)}$$

where $\gamma = \sqrt{s}/2m_Z$, $\beta = (1 - 4m_Z^2/s)^{1/2}$, $\Delta\lambda = \lambda_1 - \lambda_2$, and $\varepsilon = \Delta\sigma(-1)^{\lambda_2}$. Otherwise the notation is the same as that for $e^+e^- \to W^+W^-$ (see subsect. 3.1). The coefficients $\mathscr{A}$ are listed in table 8. Note that the divergent B terms which exist in W^+W^- production (see eq. (3.7c)) are absent here because of cancellations between the two diagrams.

Similarly for the amplitudes for $e^+e^- \to Z\gamma$ we find

$$\mathcal{M}^{(e^+e^- \to Z\gamma)} = 2\sqrt{2}\, e^2 g_{\Delta\sigma}^{Zee} \delta_{|\Delta\sigma|,\,\pm 1} \frac{\mathscr{B}_{\lambda_1\lambda_2}(\Theta)}{(1 - r^2)\sin^2\Theta} \varepsilon d^{J_0}_{\Delta\sigma,\Delta\lambda}(\Theta), \quad \text{(D.4)}$$

where $r = m_Z/\sqrt{s}$. The coefficients $\mathscr{B}$ are shown in table 8. The apparent singularity at $\cos\Theta = \pm 1$ in (D.4) is cut off by the electron mass, which leads to a finite total cross section.

In general, one may expect nonvanishing interaction of three neutral vector bosons, which contribute to V_1V_2 production via a photon or Z in the s channel. However, due to Bose symmetry and electromagnetic gauge invariance, the form of such interactions is restricted to a smaller number of couplings than in the WWV case.

For ZZ production, i.e. for two Z's on-mass-shell, Bose symmetry allows only two couplings. The most general ZZV vertex (V = Z or γ) for on-shell Z's is given by (see fig. 22)

$$\Gamma^{\alpha\beta\mu}_{ZZV}(q_1, q_2, P) = \frac{s - m_V^2}{m_Z^2}\left[if_4^{ZZV}\left(P^\alpha g^{\mu\beta} + P^\beta g^{\mu\alpha}\right) + if_5^{ZZV}\varepsilon^{\mu\alpha\beta\rho}(q_1 - q_2)_\rho\right]. \quad \text{(D.5)}$$

TABLE 8
Coefficients for the helicity amplitudes for the processes $e^+e^- \to ZZ$ and $e^+e^- \to Z\gamma$

$\Delta\lambda$	$(\lambda_1\lambda_2)$	$\mathscr{A}_{\lambda_1\lambda_2}$	$\mathscr{B}_{\lambda_1\lambda_2}$
± 2	$(\pm\mp)$	$-\sqrt{2}(1+\beta^2)$	$\sqrt{2}$
± 1	(± 0)	$\gamma^{\,1}[\Delta\sigma\cdot\Delta\lambda(1+\beta^2) - 2\cos\Theta]$	
± 1	$(0\pm)$	$\gamma^{-1}[\Delta\sigma\cdot\Delta\lambda(1+\beta^2) - 2\cos\Theta]$	$2r(\cos\Theta + \Delta\sigma\cdot\lambda_2)$
0	$(\pm\pm)$	$-\gamma^{\,2}\cos\Theta$	$r^2(\cos\Theta + \Delta\sigma\cdot\lambda_2)$
0	(00)	$-2\gamma^{\,2}\cos\Theta$	

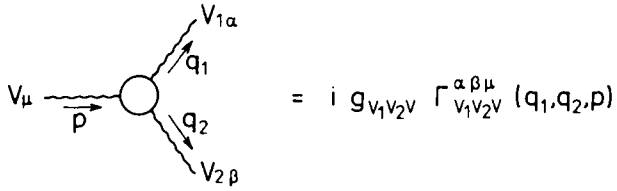

Fig. 22. Feynman rule for anomalous V_1V_2V vertices.

As in sect. 2 any terms proportional to P^μ have been neglected, since they do not contribute in e^+e^- annihilation (for $m_e \to 0$). For $V = \gamma$ such terms can restore gauge invariance, however (cf. eq. (2.10)). The vertex functions vanish at $s = m_V^2$ because of gauge invariance for $V = \gamma$, and Bose symmetry for $V = Z$. The interactions thus should come from dimension-six operators. CP invariance forbids f_4^{ZZV} and parity conservation requires $f_5^{ZZV} = 0$. If at least one of the final Z's are off-shell, five other couplings are possible, as in the WWV vertex. They are, however, proportional to $q_i^2 - m_Z^2$.

$Z\gamma$ production may have a contribution from anomalous $Z\gamma V$ couplings, where $V = \gamma$ or Z is the virtual boson in the s channel. The most general anomalous $Z\gamma V$ coupling (for on-shell Z and γ) is given by

$$\Gamma^{\alpha\beta\mu}_{Z\gamma V}(q_1, q_2, P) = \frac{s - m_V^2}{m_Z^2}\left\{ h_1^V\left(q_2^\mu g^{\alpha\beta} - q_2^\alpha g^{\mu\beta}\right) + \frac{h_2^V}{m_Z^2} P^\alpha\left(P\cdot q_2 g^{\mu\beta} - q_2^\mu P^\beta\right)\right.$$

$$\left. + h_3^V \varepsilon^{\mu\alpha\beta\rho} q_{2\rho} + \frac{h_4^V}{m_Z^2} P^\alpha \varepsilon^{\mu\beta\rho\sigma} P_\rho q_{2\sigma}\right\}, \quad \text{(D.6)}$$

where terms proportional to P^μ or q_1^α are omitted because they do not contribute to the reaction. The above expression is manifestly gauge invariant for the final on-shell photon. The couplings h_1^V and h_2^V are P-even, h_3^V and h_4^V are CP-even; all couplings are C-odd.

The overall factor $s - m_V^2$ in (D.6) comes from gauge invariance for $V = \gamma$, Bose symmetry for $V = Z$. Because of this factor, there are no corresponding operators of dimension four. If we restrict ourselves to dimension $\leqslant 6$ operators, only h_1^V and h_3^V remain; the other two receive a contribution from operators with dimension 8 and higher.

The consequences of the two dimension-six interactions in the radiative decay $Z \to \ell\bar{\ell}\gamma$ have been studied by several authors [60]. LEP-I/SLC is actually best suited to limit these couplings using radiative Z decay events. The reaction $e^+e^- \to Z\gamma$ in the presence of these couplings was discussed by Renard [59].

It is interesting to note that the four $Z\gamma Z^*$ interactions in (D.6) and the two $ZZ\gamma^*$ interactions in (D.5) are completely independent. If we keep all the three bosons off-mass-shell, there are seven couplings altogether. Four of them survive for $e^+e^- \to Z\gamma$, while two different ones contribute to $e^+e^- \to ZZ$.

The contribution of the anomalous ZZV vertex (D.5) to ZZ production can be read off from eq. (C.12) by an appropriate change of the couplings:

$$\mathcal{M}^{ZZV}(\sigma, \bar{\sigma}; \lambda_1, \lambda_2) = \frac{e g_\sigma^{Vee} g_{ZZV}}{s - m_V^2} \delta_{\sigma, -\bar{\sigma}} 2\sqrt{k^0 \bar{k}^0}\, S(\bar{k}, \Gamma_V(\lambda_1, \lambda_2), k)^\sigma_{\sigma\sigma}, \quad \text{(D.7)}$$

with

$$\Gamma_V^\mu(\lambda_1, \lambda_2) = \Gamma_{ZZV}^{\alpha\beta\mu}(q_1, q_2, P)\varepsilon_\alpha^*(q_1, \lambda_1)\varepsilon_\beta^*(q_2, \lambda_2). \quad \text{(D.8)}$$

Similar results with an obvious change of Z to γ apply for the process $e^+e \to Z\gamma$. Without loss of generality, we may choose

$$g_{ZZZ} = g_{ZZ\gamma} = g_{Z\gamma Z} = g_{Z\gamma\gamma} = e. \quad \text{(D.9)}$$

Note that the s-channel pole in (D.7) is cancelled by the zero in the couplings (D.5) and (D.6).

With all the contributing amplitudes given in eqs. (D.2) and (D.7), it is straightforward to calculate arbitrary polarized cross sections for the processes $e^+e^- \to ZZ$ and $Z\gamma$. In order to study the angular distributions and correlations of the Z decay products, one further needs the Z decay amplitudes for

$$Z(q, \lambda) \to f(p, \sigma) + \bar{f}(\bar{p}, \bar{\sigma}), \quad \text{(D.10)}$$

$$Z(q, \lambda) \to f(p, \sigma) + \bar{f}(\bar{p}, \bar{\sigma}) + g(p_g, \kappa). \quad \text{(D.11)}$$

The $Z \to f\bar{f}$ decay amplitude reads (see fig. 20a)

$$\mathcal{M}^{(Z \to f\bar{f})}(\lambda, \sigma, \bar{\sigma}) = -e \sum_{\alpha = \pm} g_\alpha^{Zff} C \omega_{\alpha\sigma}(p)\omega_{-\alpha\bar{\sigma}}(\bar{p})\alpha\bar{\sigma} S(p, \varepsilon(q, \lambda), \bar{p})^\alpha_{\sigma, -\bar{\sigma}} \quad \text{(D.12)}$$

and the amplitude with gluon radiation reads (see fig. 20b, c)

$$\begin{aligned}\mathcal{M}^{(Z \to f\bar{f}g)}(\lambda, \sigma, \bar{\sigma}, \kappa) = -e \sum_{\alpha = \pm} & g_\alpha^{Zff} g_s C' \omega_{\alpha\sigma}(p)\omega_{-\alpha\bar{\sigma}}(\bar{p})\alpha\bar{\sigma} \\ \times \Bigg\{ & \left[\frac{\varepsilon^*(p_g, \kappa)\cdot p}{p_g \cdot p} - \frac{\varepsilon^*(p_g, \kappa)\cdot \bar{p}}{p_g \cdot \bar{p}} \right] S(p, \varepsilon(q, \lambda), \bar{p})^\alpha_{\sigma, -\bar{\sigma}} \\ & + \frac{1}{2p_g \cdot p} S(p, \varepsilon^*(p_g, \kappa), p_g, \varepsilon(q, \lambda), \bar{p})^\alpha_{\sigma, -\bar{\sigma}} \\ & - \frac{1}{2p_g \cdot \bar{p}} S(p, \varepsilon(q, \lambda), p_g, \varepsilon^*(p_g, \kappa), \bar{p})^\alpha_{\sigma, -\bar{\sigma}} \Bigg\}. \end{aligned} \quad \text{(D.13)}$$

The color factors C and C' are given by (C.18). The above two formulas are applicable to any value of the fermion mass. For massless fermions, the expressions simplify significantly by the condition (C.19). The angular distribution of the final lepton for the process $e^+e^- \to Z\gamma$ in the standard model was calculated by Hayashi and Katsuura [61] and by one of us [58].

References

[1] G. Barbiellini et al., *in* Physics at LEP, ed. J. Ellis and R. Peccei, (CERN report 86-02) vol. 2, p. 1
[2] N. Cabibbo and R. Gatto, Nuovo Cim. 20 (1961) 185
[3] N. Cabibbo and R. Gatto, Phys. Rev. 124 (1961) 1577
[4] N. Van Hieu, Zh. Eksp. Teor. Fiz. 42 (1962) 1611 [Sov. Phys. JETP 15 (1962) 1118]
[5] H. Überall, Nucl. Phys. 58 (1964) 625
[6] A.D. Dolgov and V.V. Solov'ev, Yad. Fiz. 1 (1965) 860 [Sov. J. Nucl. Phys. 1 (1965) 615]
[7] Y.S. Tsai and A.C. Hearn, Phys. Rev. 140 (1965) B721
[8] O.P. Sushkov, V.V. Flambaum and I.B. Khriplovich, Yad. Fiz. 20 (1974) 1016 [Sov. J. Nucl. Phys. 20 (1975) 537]
[9] W. Alles, Ch. Boyer and A.J. Buras, Nucl. Phys. B119 (1977) 125
[10] F. Bletzacker and H.T. Nieh, Nucl. Phys. B124 (1977) 511
[11] R.W. Brown and K.O. Mikaelian, Phys. Rev. D19 (1979) 922
[12] K.J.F. Gaemers and G.J. Gounaris, Z. Phys. C1 (1979) 259
[13] M. Lemoine and M. Veltman, Nucl. Phys. B164 (1980) 445
[14] V.A. Koval'chuk and M.P. Rekalo, Yad. Fiz. 32 (1980) 1679 [Sov. J. Nucl. Phys. 32 (1980) 870]
[15] P. Mery and M. Perrottet, Nucl. Phys. B175 (1980) 234
[16] M. Gourdin and X.Y. Pham, Z Phys. C6 (1980) 329
[17] R. Philippe, Phys. Rev. D26 (1982) 1588
[18] I. Hinchliffe, *in* Proc. 1982 DPF Summer Study on Elementary particle physics and future facilities, Snowmass, Colorado, ed. R. Donaldson, R. Gustafson and F. Paige, p. 438
[19] I.F. Ginzburg, G.L. Kotkin, S.L. Panfil and V.G. Serbo, Nucl. Phys. B228 (1983) 285; (E) B243 (1984) 550
[20] P. Chen and F.M. Renard, Phys. Rev. D28 (1983) 1758
[21] R.W. Robinett, Phys. Rev. D28 (1983) 1192
[22] C.L. Bilchak, R.W. Brown and J.D. Stroughair, Phys. Rev. D29 (1984) 375
[23] V.A. Koval'chuk, M.P. Rekalo and I.V. Stoletniĭ, Pis'ma Zh. Eksp. Teor. Fiz. 40 (1984) 150 [JETP Lett. 40 (1984) 906]
[24] G. Passarino, Nucl. Phys. B237 (1984) 249
[25] V.A. Koval'chuk, M.P. Rekalo and I.V. Stoletniĭ, Z. Phys. C23 (1984) 111
[26] C.L. Bilchak and J.D. Stroughair, Phys. Rev. D30 (1984) 1881
[27] T.G. Rizzo, Phys. Rev. D32 (1985) 43
[28] D.A. Dicus and K. Kallianpur, Phys. Rev. D32 (1985) 35
[29] M.J. Duncan, G.L. Kane and W.W. Repko, Phys. Rev. Lett. 55 (1985) 773
[30] J. Maalampi, D. Schildknecht and K.H. Schwarzer, Phys. Lett. 166B (1986) 361;
M. Kuroda, J. Maalampi, K.H. Schwarzer and D. Schildknecht, Bielefeld preprint BI-TP 86/12 (1986)
[31] R. Kleiss, private communication
[32] J.F. Gunion and Z. Kunszt, Phys. Rev. D33 (1986) 665
[33] F. Olness and W.-K. Tung, Illinois Institute of Technology perprint IIT-TH/86-17 (1986)
[34] B.W. Lynn, M.E. Peskin and R.G. Stuart, *in* Physics at LEP, ed. J. Ellis and R. Peccei (CERN report 86-02) vol. 1, p. 90
[35] J.M. Cornwall, D.N. Levin and G. Tiktopoulos, Phys. Rev. Lett. 30 (1973) 1268; (E) 31 (1973) 572; Phys. Rev. D10 (1974) 1145; (E) 11 (1975) 972;
C.H. Llewellyn Smith, Phys. Lett. 46B (1973) 233;
S.D. Joglekar, Ann. Phys. (NY) 83 (1974) 427

[36] R.W. Brown, D. Sahdev and K.O. Mikaelian, Phys. Rev. D20 (1979) 1164
[37] J. Stroughair and C.L. Bilchak, Z. Phys. C23 (1984) 377
[38] M.J. Duncan, G.L. Kane and W.W. Repko, Nucl. Phys. B272 (1986) 517
[39] J. Cortés, K. Hagiwara and F. Herzog, DESY preprint DESY 85-132 (1985), Nucl. Phys. B, to be published; *in* Proc. Fourth Topical Workshop on Proton-antiproton collider physics (Bern, 1984) ed. H. Hänni and J. Schacher (CERN 84-09) p. 209
[40] M. Hellmund and G. Ranft, Z. Phys. C12 (1982) 333;
B. Humpert, Phys. Lett. 135B (1984) 179;
V. Barger, H. Baer, K. Hagiwara and R.J.N. Phillips, Phys. Rev. D30 (1984) 947;
E. Eichten, I. Hinchliffe, K. Lane and C. Quigg, Rev. Mod. Phys. 56 (1984) 579;
M. Chanowitz and M.K. Gaillard, Phys. Lett. 142B (1984) 85;
L. Roberts, Phys. Rev. D32 (1985) 701;
M. Golden and S.R. Sharpe, Nucl. Phys. B261 (1985) 217;
M. Chanowitz and M.K. Gaillard, Nucl. Phys. B261 (1985) 379;
W.J. Stirling, R. Kleiss and S.D. Ellis, Phys. Lett. 163B (1985) 261
[41] S. Weinberg, Phys. Rev. Lett. 27 (1971) 1688;
J. Schechter and Y. Ueda, Phys. Rev. D7 (1973) 3119; (E) 8 (1974) 3709; Lett. Nuovo Cim. 8 (1973) 991;
M.A. Furman and G.J. Komen, Nucl. Phys. B84 (1975) 323
[42] K. Hagiwara and D. Zeppenfeld, Nucl. Phys. B274 (1986) 1
[43] H.C. Corben and J. Schwinger, Phys. Rev. 58 (1940) 953;
T.D. Lee and C.N. Yang, Phys. Rev. 128 (1962) 885
[44] H. Aronson, Phys. Rev. 186 (1969) 1434;
K.J. Kim and Y.-S. Tsai, Phys. Rev. D7 (1973) 3710
[45] S. Brodsky and J. Sullivan, Phys. Rev. 156 (1967) 1644;
F. Herzog, Phys. Lett. 148B (1984) 355; (E) 155B (1985) 468;
M. Suzuki, Phys. Lett. 153B (1985) 289;
A. Grau and J.A. Grifols, Phys. Lett. 154B (1985) 283
[46] W.J. Marciano and A. Queijeiro, Phys. Rev. D33 (1986) 3449
[47] M. Suzuki, *in* Proc. 1985 INS Int. Symp. on Composite models of quarks and leptons, Tokyo, ed. H. Terazawa and M. Yasuè (INS, University of Tokyo, 1985), p. 138;
J.A. Grifols, S. Peris and J. Solà, DESY preprint DESY 86-055 (1986)
[48] W. Buchmüller, Acta Phys. Austr. Suppl. 27 (1985) 517
[49] H. Yamagishi and K. Hikasa, unpublished;
K. Hikasa, Masters thesis (University of Tokyo, 1980)
[50] M.E. Rose, Elementary theory of angular momentum (Wiley, New York, 1957)
[51] A. De Rújula, J.M. Kaplan and E. de Rafael, Nucl. Phys. B35 (1971) 365;
K. Hagiwara, K. Hikasa and N. Kai, Phys. Rev. D27 (1983) 84
[52] K. Hikasa, University of Wisconsin preprint MAD/PH/294
[53] K. Hikasa, Phys. Rev. D33 (1986) 3203
[54] T. Gottschalk, Nucl. Phys. B214 (1983) 201;
G. Marchesini and B.R. Webber, Nucl. Phys. B238 (1984) 1;
B.R. Webber, Nucl. Phys. B238 (1984) 492
[55] M. Tanimoto, Phys. Lett. 160B (1985) 312
[56] J.H. Kühn, Nucl. Phys. B237 (1984) 77;
J.H. Kühn, A. Reiter and P.M. Zerwas, Nucl. Phys. B272 (1986) 560;
M. Anselmino, P. Kroll and B. Pire, Phys. Lett. 167B (1986) 113
[57] K. Hikasa, Phys. Lett. 128B (1983) 253
[58] K. Hikasa, Doctoral thesis, report UT-400 (University of Tokyo, 1983)
[59] F.M. Renard, Nucl. Phys. B196 (1982) 93
[60] G. Gounaris, R. Kögerler and D. Schildknecht, Phys. Lett. 137B (1984) 261;
Y. Tomozawa, Phys. Lett. 139B (1984) 455;
V. Barger, H. Baer and K. Hagiwara, Phys. Rev. D30 (1984) 1513
[61] M. Hayashi and K. Katsuura, Prog. Theor. Phys. 62 (1979) 1781